AD NUMBER

AD436352

NEW LIMITATION CHANGE

TO

Approved for public release, distribution unlimited

FROM

Distribution authorized to U.S. Gov't. agencies and their contractors; Foreign Government Information; JAN 1964. Other requests shall be referred to The British Embassy, 3100 Massachusetts Avenue, NW, Washington, DC 20008.

AUTHORITY

DSTL, AVIA 6/24459, 23 Nov 2009

TECH. NOTE
AERO. 2944

ROYAL AIRCRAFT ESTABLISHMENT

TECHNICAL NOTE No. AERO. 2944

FURTHER DEVELOPMENTS IN LOW-SPEED WIND-TUNNEL TECHNIQUES FOR V/STOL AND HIGH-LIFT MODEL TESTING

by

John Williams and Sidney F. J. Butler

JANUARY 1964

436352

MINISTRY OF AVIATION, LONDON, W.C.2

U.D.C. No. 533.6.071.3 : 533.652.6

Technical Note No. Aero 2944

January 1964

ROYAL AIRCRAFT ESTABLISHMENT

FURTHER DEVELOPMENTS IN LOW-SPEED WIND-TUNNEL TECHNIQUES FOR V/STOL AND HIGH-LIFT MODEL TESTING*

by

John Williams
and
Sidney F. J. Butler

SUMMARY

Experimental methods for wind-tunnel testing of high-lift models with boundary-layer control and circulation control were previously described by the authors about four years ago. Some of the further advances since then, particularly those to expedite investigations on jet and fan lift models at the Royal Aircraft Establishment (Farnborough and Bedford), are discussed in the present paper. Attention is mainly concentrated on the following three selected topics:-

(a) Special mechanical and strain-gauge balance rigs for jet-blowing models;

(b) Engine exit and intake flow simulation at model scale;

(c) Ground simulation by a moving-belt rig.

The need, development and application of these techniques are considered, together with some problems still to be overcome.

*Amplified version of paper prepared for AIAA/USN Aerodynamic Testing Conference in Washington D.C. (U.S.A.) on March 9th - 10th, 1964.

CONTENTS

ILLUSTRATIONS

1 INTRODUCTION

Low-speed wind-tunnel model design and testing techniques have been continually improved throughout the years, to provide more detailed understanding and more accurate specification of aircraft performance and stability, to meet the more exacting low-speed requirements of modern high-speed aircraft, and to cope with the necessity for reduced model-scale as aircraft sizes have grown. In particular, over the past decade or so, considerable efforts have been necessary to develop specialised and novel techniques for V/STOL and high-lift model testing, including complex model and balance rig designs to allow air to be ejected from and sucked into models. Experimental methods for tunnel testing of high-lift models with boundary-layer control and circulation control (e.g. jet flaps) were last described by the authors about four years ago[1]. Some of the further advances since then, particularly those to expedite investigations on jet-lift and fan-lift models at the Royal Aircraft Establishment (Farnborough and Bedford), are discussed in the present paper.

Attention is mainly concentrated on the following three selected topics:-

(a) Special mechanical and strain-gauge balance rigs for jet-blowing models, both integral model (single balance) and composite model (multiple balance) arrangements, with air-feed connectors devised to minimise interference on balance freedoms (see Section 2);

(b) Engine exit and intake flow simulation at model scale, by separately controlled blowing and suction, by injector units, or by fans (see Section 3);

(c) Ground simulation by moving-belt rig, to check on the adequacy of the conventional fixed ground-plate with its spurious boundary layer (see Section 4).

The need, development and application of these techniques are considered, together with some problems to be overcome. There are, of course, other related topics of equal importance as regards V/STOL and high-lift model testing, including tunnel-constraint corrections, model-scale aspects, and blowing rigs for oscillatory models. Some relevant studies have been made at the R.A.E. on these further items, but time has not permitted analytic appraisal of them here.

2 RECENT JET-BLOWING RIG DEVELOPMENTS

2.1 General considerations

Balance rigs for jet-blowing models have already been discussed at some length by the authors[2,3], particularly with regard to the special air-feed connections which must be contrived between the model and the 'earthed' supply, so as to permit the required balance freedoms, yet avoid excessive interference with the mainstream flow past the model. Such considerations naturally have a major influence on the design of an acceptable test arrangement, and the demands have become more acute with the need for much greater airflow to represent V/STOL jet-lift as well as B.L.C. systems. Further advances have been made, not only in the development of low-constraint air-feed connectors, but also in devising new balance arrangements, using both mechanical and strain-gauge schemes. These include:-

(a) 'Integral' model arrangements, in which the jet nozzles form an integral part of the model, and only overall forces and moments are measured on a single balance rig;

(b) 'Composite' model arrangements, in which the direct nozzle jet-thrust effects are measured, as well as either the aerodynamic loads on the external surfaces of the model or the overall loads, using a multiple-balance rig.

2.2 Integral mechanical-balance rigs

The design of a suitable test rig for blowing models with integral jet nozzles depends to a great extent on the type of mechanical balance available. The problems are more acute with a 'conventional' balance (i.e. not platform or virtual-centre type), because the air connection has to be effected directly to the model, rather than to a platform outside the tunnel airstream. Usually, the design of a full six-component rig for blowing models is extremely difficult with the conventional balance, whereas three-component rigs can readily be contrived for longitudinal force and moment measurements. A half-model technique with a reflection plane is then often adopted because of the advantages of simplicity and scale.

The development of low-constraint air-feed connectors for conventional and other balance rigs has continued. At R.A.E., air-bearing connectors have been extensively and profitably employed on many types of blowing and suction models, as described in the earlier paper. As an alternative, labyrinth-seal connectors have also been applied, for example to a horizontal half-model rig in the 13 ft x 9 ft tunnel with a conventional overhead balance (see Fig.1). In addition, multiple P.V.C. tube connectors have been used to effect simple air-feed connections without any leaks for pressures up to 5 atmos. abs., as in the three-component complete-model rig[4] of Fig.2. With careful adjustment, it has been shown that the ensuing balance constraints can be reduced to acceptable levels with adequate repeatability. Further developments to higher pressure-ratios are contemplated, with suitable reinforcement of the tube strength.

In the original R.A.E. six-component virtual-centre floor balance rig, a single central vertical support strut was employed, with an air-bearing connector arrangement to the balance platform[3]. Similar rigs have now been devised with equal success for other virtual-centre balances elsewhere. Meanwhile, the R.A.E. rig has been used extensively for tests of V/STOL blowing and suction models, including extensive ground effect measurements (see Section 4). The associated air-bearing connector has recently been redesigned (Fig.3) to permit the use of increased air-feed pressures up to 10 atmos. abs. (instead of the original 5 atmos. abs.), still preserving an adequate yaw range (now ±25°); pneumatically-operated seals were also incorporated to allow accurate mass-flow checks inbetween balance measurements. Other types of air-feed connectors could, of course, be substituted for this air-bearing, provided a suitable turntable arrangement were employed; with good design and careful adjustment, balance constraints should still be repeatable and within acceptable limits.

2.3 Composite rigs

With B.L.C. and circulation control models, where there is considerable lift augmentation, reasonable test accuracy has proved possible with overall balance measurements on integral models, assuming careful jet-flow calibrations. However, considerable difficulties have been encountered with powered V/STOL models when only overall balance measurements have been available. In order to determine comparatively small aerodynamic interference effects with sufficient accuracy, the engine thrust has to be determined most carefully, with due allowance for possible variations with forward speed and model condition. Ideally, measurements of the external aerodynamic loads (excluding engine thrust), together with either engine thrust or overall force measurements, are required. Hence, some practical arrangements are now being developed, initially in conjunction with the existing virtual-centre balance rig, to facilitate such measurements at R.A.E. on V/STOL models with round jets.

One model, with fuselage jets, is to be tested with an internal strain-gauge balance supporting the wings and the fuselage. This balance, together with the fuselage jet nozzles, is then supported by the variable-incidence head of the usual central strut of the virtual-centre balance (Fig.4). Thus, overall balance measurements can be obtained as well as the measurements of the 'aerodynamic interference' loads on the wing and fuselage (excluding the nozzle exits). Naturally, investigations will be necessary of the problems associated with sealing the nozzle fairing junctions, with leaks, and with possible spurious loads on internal surfaces. Provided such difficulties can be adequately surmounted, the internal strain-gauge balance can profitably be employed for such 'interference-type' tests of this model in other tunnels, where a suitable mechanical balance rig for overall measurements is not readily available.

The jet-nacelle model described in Section 3.5 presents rather different problems, since the round jets are here located below the high-lift wing, in external engine nacelles (Fig.5a). The incorporation of individual balances with integral air-feeds in the supporting pylons would have been attractive, but was not considered practicable in view of the small scale. Moreover, to ensure adequate derivation of wing load changes, the nacelle load measurements would need to be comparable in accuracy with the overall load measurements on the main balance. Therefore, the overall balance measurements (with the engine nacelles attached to the model) are instead to be supplemented by 'interference' measurements with the engine nacelles separately supported in an inverted position from the tunnel overhead balance to provide nacelle lift and thrust, and with the remainder of the model (inverted) on the main floor balance (see Fig.6). These latter measurements will necessarily be limited to fixed incidences and zero yaw, while there are admittedly difficulties concerned with alignment, deflection, and possibly rig interference. However, there is some compensation in the facility for wide variations of the engine nacelle position relative to the wing.

2.4 Strain-gauge balance problems

Unless a good platform balance is available, strain-gauge balance rigs may well be preferable for V/STOL models, particularly for six-component measurements. The possibility of a variety of support arrangements is attractive from tare and interference considerations, the balance can be designed to

suit individual model requirements, and comparative tests in different tunnels are facilitated. S.G. balances are also useful for auxiliary measurements, such as control hinge moments, nacelle loads, etc.

Nevertheless, there are considerable reservations concerning S.G. balances from our point of view, particularly as regards balance interactions, low sensitivity, zero drift, and model safety. Thus, unlike well-designed mechanical balances, multi-component S.G. balances inevitably suffer from significant interactions and a special calibrating rig is usually necessary, with periodic checks of the main interactions as well as the direct calibration. Balance sensitivity, essentially defined by the specified working range, is necessarily rather low, say 1 part in 2000 of maximum load, but this is probably adequate if the model and balance are well-matched. Unfortunately, lower sensitivity than usual must be expected for V/STOL models, as a result of the need for a generous safety factor to allow for difficulties with model load estimation, particularly under stalling conditions. Zero-drift can also be troublesome, even when the gauges are carefully selected, positioned, and attached, with temperature compensation applied to each bridge. In view of the rather low overall accuracy which seems likely, it therefore appears advisable to employ interference rigs (see Section 2.3) where practicable.

S.G. balance units should be located near to or preferably inside the model, to minimise deflections and force interactions on moments, and to achieve good moment accuracy. Although the design considerations for a rear-sting internal or external balance may otherwise not differ materially from those encountered with high-speed tunnel models, tare and interference considerations can be particularly involved for V/STOL models with a rear support arrangement. As an alternative, when room is available, a similar balance design with a vertical support strut may be adopted. Tare and interference effects are rather easier to handle, both because the moment arms concerned are smaller and because their determination by a dummy strut technique is then feasible if the model can also be inverted on its strut. It is necessary, of course, to guard against the possibility of strut-induced separations, and to assess the magnitude of the interference on the flow over the fin and the tailplane.

For recent six-component tests in the R.A.E. 24 ft (diameter) tunnel* on a propeller slipstream model with blown T.E. flaps[5] (see Fig.7), an internal five-bar horizontal cage balance was arranged above a faired external three-bar drag unit, the whole assembly being mounted on a braced vertical support tube attached to the tunnel turntable (Fig.8). Small amounts of compressed air for B.L.C. purposes (up to $\frac{1}{2}$ lb/sec at 3 atmos. abs. and temperatures up to 5°C above ambient) were conveyed through the balance to the model, via the central hollow members of each balance cage, without significant effects from internal temperature and pressure on balance zeros or calibration. However, a test with higher flow rates (some $2\frac{1}{2}$ lb/sec) at 20°C above ambient showed large zero drifts, especially for the gauges directly mounted on the air ducts, and implied that temperature gradient effects could lead to serious difficulties in the stabilisation of zeros. Generally, it seems preferable to effect such air connections separately, using low-constraint pressurised connectors on which experience is already accrued, possibly with some insulation of the balance against heating effects.

*This tunnel has not got a six-component mechanical balance.

If an external S.G. balance arrangement proves necessary, it may conveniently form part of a suitably-shielded vertical support strut. Such an arrangement is proposed for R.A.E. 24 ft tunnel tests on the jet-nacelle model, a five-component sting balance being incorporated in the length of a hollow elliptic tube constituting the central portion of a vertical support strut. Moments about the model centre will be derived from gauge stations at which the cross-sectional areas are proportional to distance from the centre, the forces from gauge stations with equal areas. Lift is to be measured separately by the existing mechanical balance on which the whole assembly is to be mounted. The hollow, tubular design for the S.G. balance ensures maximum rigidity and affords accommodation for separate air-supply connections, which will be effected so as to minimise balance constraints. In view of the large quantities and pressures to be considered (up to 10 lb/sec at 10 atmos. abs.), a mock-up tubular balance of circular cross-section has been constructed to investigate connector constraint, as well as to assess the need for insulation between the air supply and the balance in order to avoid temperature gradients and zero drifts.

3 JET EFFLUX AND INTAKE FLOW SIMULATION

3.1 Basic considerations

For a specific model and jet exit geometry, model attitude, and jet inclination, the aerodynamic interference effects between the jet efflux and the mainstream flow past the airframe surfaces can be correlated non-dimensionally against a momentum-ratio or effective speed-ratio $\sqrt{\rho_o V_o^2/\rho_J V_J^2}$; here, V_o and V_J are the relevant mainstream and jet velocities, while ρ_o and ρ_J are the corresponding densities. From our experience at model-scale, the further influences of jet Reynolds number $R_J(\equiv V_J d_J/\nu)$, of jet to mainstream temperature ratio and of jet pressure-ratio appear to be of second order, though some precise measurements with jet conditions nearer to full-scale in both size and temperature are still needed to qualify these assumptions. Equally well, a jet-momentum coefficient $C_J[\equiv J/q_o S]$ can be employed as the primary correlation parameter, where J represents the rate of ejection of momentum, q_o is the mainstream dynamic head and S is a planform area. But this must not be taken to imply that the relative size of the jet exit to the surrounding planform is unimportant, as usually assumed with thin jet sheets for blowing B.L.C. and jet-flaps. In fact, aerodynamic interference effects have been found to vary markedly, for example, with the proportion of aircraft planform area occupied by the jet exits, the disposition of the jet exists in the planform, and the height of the airframe lower surfaces above the nozzle exits. The efflux velocity distribution may also be significant, though so far we have not explored this effect.

The influence of intake suction on the flows over neighbouring airframe surfaces can perhaps be usefully envisaged as arising from a distribution of sinks over the intake face, provided the front lip radius and entry design are adequate to preclude significant flow separation. For a prescribed aircraft geometry and intake location, the major parameter as regards associated

interference effects seems likely to be the intake flow-rate coefficient $C_Q[\equiv M_s/\rho_o V_o S]$, where M_s represents the mass flow rate of mainstream air into the intake duct. Although there is yet no real justification to assume that the distribution of the sink strength across the intake face or the proportion of the surrounding planform occupied by the intake can entirely be ignored, reproduction of the exact intake shape and size does not seem so important as for the jet exit. In fact, for our purposes, modification of the intake geometry is sometimes desirable to preclude spurious flow separation on the intake lip at model Reynolds numbers, though the location of the intake should be altered as little as possible. Of course, intake design studies in relation to specific engine or fan performance and internal flow considerations will tend to require correct representation of the intake shape and associated flow control devices, but the scale should then be as large as possible. Furthermore, this may also apply for the investigation of external aerodynamic interference effects, if the practical full-scale intake has to tolerate flow separations under some operational conditions.

Blowing nozzle and duct design problems for jet-lift V/STOL aircraft are discussed in Section 3.2, their treatment being illustrated by reference to simple jet-wing and jet-fuselage models, a one-tenth scale Hawker P.1127 model and the R.A.E. subsonic-transport jet-nacelle research model. The further provision of intake suction can be tackled in a variety of ways depending on the configuration and the purposes of the test programme. Separate ducts for the intake and exit flows are incorporated in the Hawker P.1127 model (Fig.9), but the feasible intake flow rates are rather small. The suction ducting problems become even more intolerable when nacelle installations are involved. Fortunately, for research purposes at least, correct matching of intake and exit flow rates to simulate specific lifting units is not essential, provided comparative tests are also made with similar exit flows but no intake flow. Special injector nacelle units, devised to produce intake and exit flows adequate for basic and applied research at speeds about half full-scale, are discussed in Section 3.3. The corresponding application and development of some model fan units is next outlined in Section 3.4. For completeness, the overall design and construction aspects arising with representative jet-lift V/STOL aircraft models are illustrated by a brief description in Section 3.5 of the general scope and layout of the jet-nacelle model.

3.2 Blowing duct and nozzle design

With jet-lift V/STOL models, the ducting of air to the blowing nozzles becomes more difficult than for the B.L.C. and jet-flap models previously considered, because the air mass flows involved tend to be much larger, while the nozzle lengths have to be severely restricted - often to two diameters or less. Furthermore, to minimise the size of the supply strut to the model for aerodynamic tare interference reasons, the dynamic head of the air entering the model tends to be large and needs to be destroyed or dispersed. However, if the space inside the model is large enough to provide a low-velocity plenum duct, followed by a pressure-drop and a contraction into the final nozzle, then a uniform and steady jet efflux should readily be feasible. More generally, there is less room available in the model or the air-flow rates are appreciably larger, so that the problems not only become more difficult but also specific to the model in question; however, some general principles are still worth mention. Firstly, a pressure chamber can usually be profitably employed, where

feasible, with the air at high pressure (high density) to minimise volume flow rates at the strut entry and inside the chamber. Again, to suppress any large local velocities or high swirl inside the chamber arising from the necessarily high dynamic head at entry, baffling is needed according to the nozzle configuration under test. A contraction should also be incorporated ahead of the nozzle exit wherever possible, preceded by resistance screens at the contraction entry, to improve the nozzle flow distribution and to regulate the pressure ratio across the nozzle.

For example, an early simple jet-wing model[6] of rectangular planform (30 in. x 27 in.), which was mounted inverted on a vertical supply strut, included a pressure box of $1\frac{1}{2}$ in. internal depth. The variety of jet exit arrangements in the test surface ranged from multiple holes of either $\frac{1}{2}$ in. or 1 in. diameter to a single central hole of $2\frac{1}{2}$ in. diameter. Apart from a simple baffle gauze in the box opposite the air-supply entry (see Fig.10a), no elaborate internal schemes were needed to ensure practically identical efflux flows from the different holes of the multiple jet arrangements, which were drilled directly through the 1 in. depth of the surface plate. Improvement of the uniformity of the velocity distribution across each jet exit could have been achieved with a convergent instead of a parallel hole. With the mass-flow rate limited to about 1·3 lb/sec, the dynamic pressure at the entry to the model was about 0·2 atmos. and the total pressure about 1·75 atmos. abs., providing a nozzle exit pressure ratio as high as 1·6/1 because of the small losses in the plenum chamber. For the tests with a single hole of $2\frac{1}{2}$ in. diameter directly opposite the strut entry, the wing pressure box was of no material advantage. Although an acceptable efflux distribution was achieved by the use of a short contraction with a resistance gauze at the entry, the available pressure ratio across the exit nozzle was substantially reduced.

On a simple fuselage-jet delta-wing model[7], one to four nozzles of diameters ranging from $1\frac{1}{4}$ in. to $2\frac{1}{2}$ in. were located in the base of a pressure chamber ($3\frac{1}{2}$ in. internal depth) forming the central part of the fuselage (Fig.10b). With the maximum mass-flow rate of 3·25 lb/sec, the dynamic pressure at the entry to the model reached 0·75 atmos., with an entry total pressure of about 3·5 atmos. abs., providing a jet exit pressure-ratio of about 1·9/1. Acceptable efflux distributions, usually within ±5% of the mean jet velocity, were attained by the incorporation of baffles opposite the flow entry, together with resistance gauzes and contractions ahead of the nozzles; but this is not to dispute the difficulties involved.

In the one-tenth scale Hawker P.1127 model[8], no proper plenum chamber was feasible, so the air supply from the vertical strut was divided to provide individual duct feeds directly to the four rotatable nozzles (Fig.9). With the maximum model mass-flow of 4·25 lb/sec, the air entered the model with a dynamic pressure of 0·75 atmos. and a total pressure of 3·5 atmos. abs., the jet exit then running almost choked. To ensure representative jet efflux conditions, each nozzle had an area contraction of about 1·3 to 1 in. in the final turning cascade, and two sets of resistance gauzes were incorporated upstream.

For the jet-nacelle model, the air ducting problem again becomes particularly acute, since the jet-engine nacelles have to be attached to the wing by representative slender pylons (Fig.5a). In this model, each main wing constitutes a pressure box designed to pass 5 lb/sec at 10 atmos. absolute through

the hollow pylons to the engine nacelles. Typically, the velocities inside the wing duct and pylon can be as large as 600 ft/sec. The engine nacelles serve as pressure chambers, but a variety of internal baffle arrangements have proved necessary according to the exit nozzle configuration. Thus, good exit distributions were ensured for double and quadruple side-nozzle arrangements, by incorporating a V-shaped partially perforated baffle opposite the pylon entry, together with gauze-covered contractions of 1·6/1 ahead of the nozzles (Fig.11). Typically, with one quadruple-nozzle nacelle on each wing, the variation of local velocity across the exit of an individual nozzle was within ±5% of the mean exit velocity, while the variation of mean exit velocity for the eight nozzles did not exceed 3%. However, in the case of the single large-nozzle nacelles, no such contraction was feasible and baffling arrangements were less satisfactory. To obtain an acceptable efflux distribution, it was necessary to insert a honeycomb in the nozzle, preceded by a special perforated plate, individually graded by experiment for each particular nozzle.

3.3 Injector units

Some compromise is necessarily involved in the design of injector units with compressed air as a primary source*, for the simultaneous representation of both the exit and intake flows in jet-lift nacelles (e.g. Fig.12). Two flow limitations must be accepted from the outset, though fortunately these appear to be of secondary importance as regards aerodynamic interference effects (see Section 3.1). Firstly, the exit flow temperature from the injector unit is, of necessity, close to ambient, so jet efflux temperature effects are not simulated. Secondly, as discussed later, reduced exit velocities (or total pressures) have to be accepted if reasonable amounts of intake flow are to be induced by the injector, so the mainstream speed needs to be lowered to cover the appropriate speed-ratio range. The acceptable reduction in jet efflux and mainstream speeds is also governed by the requirement for sufficiently high values of nacelle thrusts and model loads to ensure adequate accuracy of measurement.

The mass-flow ratio (induced/primary) required from an air injector at near-ambient temperature, to simulate both the appropriate engine intake mass-flow coefficient $(M_s/\rho_o V_o S)$ and the effective jet-speed ratio $(V_o/V_J)(\rho_o/\rho_J)^{\frac{1}{2}}$ with the scaled exit area, is approximately proportional to $T_o^{\frac{1}{2}}/(T_J^{\frac{1}{2}} - T_o^{\frac{1}{2}})$, where T_J denotes the full-scale engine jet temperature and T_o the ambient temperature. Typically, this injector mass-flow ratio may rise from about 1·2 to 3·2 as the corresponding full-scale efflux temperatures are reduced from 1000°K to 500°K. Such small mass-flow ratios may not seem large, compared with values for more conventional applications. But the total pressure rise to be imparted to the inlet air tends to be much larger here than usual, because the exit velocities have to be kept high enough to produce adequate thrusts and model loads. A further major design problem is the requirement for a reasonably uniform distribution of exit velocity after only a short mixing section inside the injector unit. Fortunately, experimental studies on a variety of multiple primary nozzle arrangements[9] have shown that practical solutions are possible.

*Hydrogen peroxide rockets, with or without kerosene burning, offer a hot jet efflux but these are not acceptable for unrestricted testing in our return-circuit tunnels with closed wooden working-sections.

To explore possible performance limits, some theoretical curves derived from un unpublished analysis on injectors by M. Lopez of English Electric Aviation Ltd. (B.A.C., Warton Division) may profitably be used, since little experimental evidence on injector efficiency and optimisation seems to be available over the region of our special interests. In Fig.13, the injector mass-flow ratio is plotted as a function of the primary parameter $(P_{o1}/P_4)(1/A_R)$; P_{o1} represents the primary flow stagnation pressure, P_4 is the ambient static pressure at the end of the mixing tube, and A_R is the ratio of the cross-section area at the mixing tube to the exit area of the convergent primary nozzle. The resulting curve, together with the optimum value of this primary parameter as regards maximum mass-flow ratio, is then solely a function of the secondary parameter $(1 - 1/A_R)(P_{o2}/P_4)$; P_{o2} signifies the stagnation pressure of the induced flow. Clearly, an increase in pressure-ratio P_{o1}/P_4 is theoretically always beneficial, since the area ratio A_R needed to achieve a prescribed value of the primary parameter is reduced, so that the secondary parameter and hence the mass-flow ratio tends to increase. Furthermore, when the primary parameter is above its optimum, an increase in area ratio leads to a higher mass-flow ratio from two aspects, since the primary parameter decreases towards its optimum while the secondary parameter again increases. The supplementary curves for the secondary flow Mach number, M_3, are also instructive in indicating the Mach number at the end of the mixing tube, though strictly they refer to conditions near the position of the primary nozzle throat. Unfortunately, large values of the mass-flow ratio are accompanied by correspondingly low values of the exit Mach number. Thus, for mass-flow ratios in excess of 2, exit Mach numbers of 0·6 or less are likely, depending on the degree of optimisation and the maximum pressure-ratio available.

In practice, the injector performance naturally falls below theoretical estimates due to intake losses and viscous effects, even when an adequate mixing length is available. The limited experimental evidence on simple injectors within the mass-flow and exit velocity range of present interest suggests that viscous effects reduce the feasible mass-flow rates by some 10% and that the optimum is achieved at values of the primary parameter somewhat higher than theoretical estimates.

The model injector nacelle unit shown in Fig.12 comprises essentially a cylindrical mixing tube surrounded by an annular reservoir supplying compressed air forward to the primary nozzle exits. The latter here consist of a 'cartwheel' spoke arrangement of elliptic tubes, each with a blowing slot at its trailing edge. Some primary air is also fed to a peripheral slot, to ensure unseparated flow against the adverse pressure gradients at the cylinder wall and to maintain adequate velocity there. This arrangement gives steady and uniform flow, the spatial variations in local exit velocity being within ±5% of the mean. At the design pressure-ratio of about $3\frac{1}{2}$ atmos. abs., a mean velocity of nearly 650 ft/sec is attained. However, the mass-flow ratio (induced/primary) is only about 0·8 which, while adequate for research purposes, gives inadequate intake flow for representative lift-engine simulation. Any radical improvements would necessitate significant reductions in primary nozzle area, leading to exit velocities of 500 ft/sec or less with the existing primary pressure-ratios. Further experimental research might permit design arrangements with even shorter mixing length, without impairing performance or the uniformity

of the exit flow distribution. Fortunately, as would be anticipated theoretically, the performance of the present injector units does not appear to be sensitive to external flow changes within the normal test range. However, with more efficient injector units and more representative mass-flow ratios, increased sensitivity seems likely, so that careful calibration over the whole range of mainstream test conditions would then be advisable.

The current injector units are being employed to provide simultaneous inlet and exit flows on the jet-nacelle research model, as described in Section 3.5. The measured aerodynamic interference effects will be compared with results for nacelles with similar exit efflux but no intake flow. For the future, adequate representation of lift engines such as the R.B.162 should be feasible down to 1/15th or 1/20th model scale. Representation of lift/thrust units with multiple rotating nozzles presents a difficult problem, because the intake flow has to be divided accordingly, without incurring pressure losses which would reduce the injector performance. These difficulties become even more acute if large bypass-ratios without plenum chamber burning have to be simulated. Much further experimental work on possible units is therefore necessary towards this end.

3.4 Model fan units

At the R.A.E., model fans have been employed simply as convenient methods of providing simultaneously both upper surface intake suction and lower surface jet efflux, for basic research investigations on associated aerodynamic interference effects at forward speeds; the representation of specific full-scale lift-engine or lift-fan units is not intended. Thus, while variations in fan power are of some interest, the measured momentum flux and mean velocity of the fan duct flow have primarily been employed for the correlation of results from both balance measurements and detailed surface pressure-plotting. Further, to derive the effects due to adding intake flow, some comparative tests have also been made on similar models with only the jet efflux represented.

In early experiments[10,11], electric motors had to be used to drive simple fans (or ducted propellers), but the available power/size ratio gave inadequate efflux velocities for accurate measurements at low practical values of mainstream speed/jet speed, while the installation space required in the model was unduly large compared with the duct internal diameter. Special compact units had therefore to be developed to allow simulation of practical groupings of lift-engines or fans, e.g. in-line along a nacelle or wing, and to permit a more representative proportion of the nacelle or wing planform areas to be occupied by duct exits.

Air-driven fan units, with a casing width not much in excess of the fan diameter and an axial depth even less, seemed to offer an attractive and feasible approach. Mean efflux velocities of at least 300 ft/sec were essential to ensure reasonable tunnel testing speeds and model loadings, while air-supply pressures had to be limited to about 4 atmos. abs. to match the compressor equipment available. Two sizes of air-driven fan units were therefore designed and built by Dowty-Rotols Ltd. to meet these R.A.E. requirements, a 6 in. diameter fan intended for basic research on nacelle (or fuselage) installations,

and a 3 in. diameter fan of minimum depth for both wing and nacelle installations. Unfortunately, due to unforeseen delays in the production of these novel units, most of our wind-tunnel investigations have so far had to be made with existing electrically-driven fan units. But it seems worth outlining the recent experience with the air-driven fans at R.A.E. Bedford, in conjunction with Dowty Rotols.

The 6 in. diameter fan consists of four aerofoil section blades mounted in the hub so that the blade angles can be adjusted to any required setting (Fig.14a). The axial-flow impulse-type turbine wheel is mounted integrally with the fan hub, the air being fed to the wheel via an annular volute forming part of the fan casing, and thence through three hollow spokes and a central chamber to a set of stationary nozzles immediately above the turbine wheel. The turbine exhaust then passes over the fan blade roots and mixes with the fan efflux, all of which finally passes through a set of outlet guide vanes. There is a tachometer unit integral with the outlet guide vane assembly to indicate fan r.p.m. The installed size of the whole fan unit is approximately 8 in. square by 6 in. deep - inclusive of a 1 in. inlet radius. The units can thus be mounted in line at a pitch of only 1·33 times the fan diameter, provided space is available for an air-supply inlet manifold.

The production 6 in. fan yields a thrust of about 44 lb at the rated r.p.m. of 36,000, when it requires an air-feed of 0·8 lb/sec at 3 atmos. abs. and ambient temperature, the mean velocity of the efflux then being slightly greater than 300 ft/sec. It is worth noting that the fan performance is below design estimates primarily because large pressure losses occur in the intake flow past the three spokes delivering air to the hub turbine. Unfortunately, the velocity distribution in the efflux is far from uniform, so that reliable efflux surveys are difficult. Due to the high tip-speed of the fans (940 ft/sec), the noise level is high, requiring the use of ear protectors by test personnel. However, with the model fans inside a closed wind-tunnel, quite elementary noise insulation seems to reduce the noise to acceptable levels in surrounding areas. The fans have otherwise proved easy to operate and the r.p.m. appears to be insensitive to changes in cross-flow velocity (for $V_o/V_J <$ 0·5 at least) and also to model incidence changes, at least for four fans in-line along a nacelle.

The 3 in. diameter fan is provided with a peripheral turbine drive because of its small size (Fig.14b). The fan comprises eight fixed aerofoil-section blades mounted integrally in the turbine wheel, the drive air being fed to the turbine from an annular duct forming part of the fan casing, via nozzles with inlet guide vanes. Outlet guide vanes are fitted to both the fan efflux and turbine exhaust, while the fan r.p.m. is indicated by a tachometer integral with the fan hub assembly. The installed size of the whole fan unit is approximately 6 in. square by 3 in. deep - inclusive of an inlet radius; the units can be mounted in-line at a pitch of twice the fan diameter.

At the present stage of development, this 3 in. fan unit yields a thrust of 9 lb at an r.p.m. of 55,000, requiring an air-feed of about 0·4 lb/sec at a pressure of 4 atmos. abs. and ambient temperature; for reasons not yet known, the fan performance is not up to design expectation. Since the blade tip-speed only reaches 720 ft/sec, the noise tends to be much less noticeable than with the 6 in. fan. Tunnel model tests await the delivery of a sufficient number of these 3 in. diameter fan units.

3.5 Jet-Nacelle Model design

Accumulated design experience with planar and round jet models can usefully be illustrated by discussing the design and construction of a complex subsonic transport jet-nacelle research model now being extensively tested[13] at R.A.E. This has a high aspect-ratio wing of moderate sweep back, with blowing B.L.C. over both leading-edge and trailing-edge flaps. Propulsive, lift/thrust and pure-lift jet units can be disposed in underslung nacelles, to simulate both elementary and practical engine arrangements (see Fig.5a). Although the aerodynamics of the basic B.L.C. wing are of considerable fundamental interest, the main investigations will concern the effects of the engine jet efflux and (to a lesser extent) intake flows on the aerodynamic efficiency of the wings and flaps, including minimum blowing momentum coefficient requirements for B.L.C., as well as of the influence of the modified flow around the wing, fin, and tailplane on stability.

The first tests are being made with the model mounted on the virtual-centre jet-blowing rig of the R.A.E. No.2 11½ ft × 8½ ft tunnel; jet-nacelle 'interference' measurements (see Section 2.3) will be made with the nacelles separately supported from the overhead balance, as well as overall measurements with the nacelles attached to the wings. Ground effect measurements using a conventional fixed ground-plate can be checked using the Moving-Belt Ground Rig as deemed necessary (see Section 4). To investigate constraint and blockage aspects, comparative tests are to be made subsequently in the larger 24 ft diameter tunnel, using a strain-gauge balance arrangement (see Section 2.4).

The wing has a constant 13% thick R.A.E. 102 cambered section and a mean chord of 10 inches, and is of aspect ratio 8 with a taper ratio of 0·5 and 28° L.E. sweepback. As well as the basic undeflected and unblown L.E., a full-span 12½% L.E. flap is provided with knee blowing at settings of 30° and 40° (normal to the hinge-line). Knee blowing is also incorporated in the 25% T.E. flaps and ailerons, for settings of 40°, 60° and 80°, in addition to the unblown and undeflected T.E. flap. For structural rather than aerodynamic reasons, the B.L.C. ducts were accommodated within the flaps, to make best use of the available wing volume, with a supply of up to 0·7 lb/sec at 3 to 4 atmos. abs., through a pair of 7/8 in. diameter pipes incorporated in the model support strut (see Figs.5a,b). Because of the B.L.C. nozzle widths involved (0·002-0·004 in. at L.E., 0·004-0·008 in. at T.E.), careful design was necessary to minimise slot distortion under internal pressure, including the acceptance of an inclined nozzle rather than tangential blowing. The nozzle width is regulated by graded spacers, located ahead of the final contraction from nozzle blockage considerations. The design has proved successful, with tolerable nozzle width variations under pressure (generally not exceeding 10%), good balance between the two wings, and satisfactory spanwise total head distributions.

With the rig for overall force and moment measurements, the main compressed air supplies for engine representation are introduced via two remotely-controlled motorised valves at the base of the strut, connected to the main two-inch diameter strut tubes. At the strut head, each of these ducts is divided to supply one duct of each wing, with a special "O"-ring seal arrangement to avoid leaks over the required incidence range. Each wing is

constructed from upper and lower machined steel members, joined on the wing chord plane to form two distinct spanwise ducts. Quite separate air supplies can thus be provided to inboard and outboard nacelles, with provision for interconnection to minimise duct pressure losses when only one engine supply is required. Engine mounting positions and duct exits are provided at various spanwise stations, including the tip.

In the design and manufacture of the wings, it proved quite difficult to ensure maximum duct area whilst retaining sufficient strength to withstand the internal pressure and adequate stiffness to avoid excessive tip deflections under aerodynamic load. Careful manufacture was necessary, with heat treatment and straightening between successive stages of internal and external machining. However, with a supply pressure of 10 atmos. abs., a total flow approaching 10 lb/sec has been achieved with an adequate usable nacelle pressure of 5 atmos. abs.

As regards engine arrangements, pairs of $2\frac{1}{4}$ in. diameter simple ejector nozzles are provided, for attachment at 25%, 35% or 45% semispan, representing elementary 0° and 90° lower surface jet sources. By adding fairings, these nozzles can be converted into the corresponding ejector nacelle configurations for comparative purposes. The injector nacelles (with partial intake flow representation) and the ejector nacelles (no intake flow) can also be mounted at the same spanwise stations on pylons affording three clearances, with an alternative chordwise position at the middle clearance. The injector nacelles, with alternative intake lengths, have 0°, 30° or 90° rear nozzles of $2\frac{1}{4}$ in. diameter, and are each capable of exit velocities approaching 700 ft/sec and a thrust of some 33 lb. The ejector nacelles can be fitted with the rear nozzles, or with single lower nozzles, or with either one or two pairs of swivelling side nozzles, each configuration having a total nozzle area of 4 sq in. With the side nozzles, each ejector nacelle can produce a thrust of about 70 lb at a jet speed of about 1000 ft/sec.

For lift-engine representation, multiple injector and ejector nacelles have also been designed for attachment at 60% and 80% semispan, or at the wing tip.

4 GROUND SIMULATION BY MOVING-BELT RIG

4.1 Nature of problem

With modern high-lift systems and V/STOL aircraft, ground effects are often large and sometimes adverse. The need has arisen to check the adequacy of relevant wind-tunnel tests with the conventional fixed ground-plate since unrepresentative boundary-layer flows occur on the ground-plate. Removal of this boundary layer can be ensured by suction through the plate, but the quantity of air involved tends to be so large that extraneous 'sink' effects are superimposed on the whole flow field between the model and the simulated ground. Furthermore, the choice and control of the suction inflow distribution tends to be particularly difficult and critical over local areas where strong pressure gradients are present. Another technique requires a second 'image' model inside the tunnel working section, without an intermediate ground-plate, providing a symmetrical flow pattern above and below the free boundary. However, aerodynamic justification of this technique is difficult when appreciable ground effects are expected, particularly if strong vorticity or jet flows are present.

Again, there is a real difficulty in ensuring precise similarity in the aerodynamic behaviour of the two models under high-lift conditions. Perhaps a more natural approach to practical conditions is to eliminate the spurious relative motion between the fixed ground and the mainstream, though admittedly this is not a simple task if a satisfactory installation for research work is the aim.

An elaborate moving-belt ground rig has been developed at R.A.E.[12], essentially consisting of an 8 ft wide continuous belt, running at speeds up to 90 ft/sec over a pair of rollers of 1 ft diameter located $9\frac{1}{2}$ ft apart, installed in an $11\frac{1}{2}$ ft × $8\frac{1}{2}$ ft tunnel. The rig was designed primarily for use with existing and new models mounted on the floor virtual-centre balance, which has a special air-connector system to expedite testing of jet-blowing models on a single vertical-strut mounting. For our purposes, therefore, it was preferable to mount such models upside down in the tunnel, with the moving-belt ground above them (Fig.15). But the general description and comments which follow in Section 4.2 should apply equally well for an upright model with the ground rig below it.

An aerodynamic appraisal of essential ground test techniques, especially as regards the adequacy of the conventional fixed ground-plate approach, is in progress at R.A.E. using a wide range of models on the moving-belt rig. Some early comparisons from the experiments completed to date are mentioned in Section 4.3.

4.2 Moving-Belt Rig design

4.2.1 Structural features (Fig.16)

The metal supporting structure comprises frames in weldable aluminium, the two side frames and the bracing cross frame being bolted together. The rollers, which are 8 ft wide and made from 3/8 in. mild steel plate, rolled and machined to $\frac{1}{4}$ in. thick, are attached to a solid steel shaft (3 in. diameter) by a central as well as end fittings, to preclude shaft whirling. The amount of roller camber needed to ensure flat running of the belt against the plate proved rather smaller than anticipated, namely linear taper from a constant $12\frac{1}{2}$ in. diameter over the central 3 ft span to $12\frac{1}{4}$ in. diameter at the ends. The rollers, pitched a distance 9 ft 6 in. apart, have three of the four end bearings in longitudinal slides, each with an auxiliary motor driving a screw jack for adjustment. This permits as much as 5% extension lengthwise to ensure adequate belt tensioning, to cope with permanent elongation and to provide differential tensioning for effecting tracking control.

The main roller drive is at the fixed end-bearing, with the power supplied by a 20 h.p./400 volt A.C. motor located above the tunnel, through a manually-operated variable-speed V-belt pulley system. There is a vertical keyed shaft, a spiral bevel box (1/1 ratio), a magnetic clutch and a grooved pulley drive (1·7/1 speed increase).

The endless moving belt, made from standard 3-ply material, of overall thickness 3/16 in. and weight 32 oz/sq yd per ply, is 7 ft 10 in. wide and 22 ft long. There is a longitudinal seam because of the large width, but the

constructed from upper and lower machined steel members, joined on the wing chord plane to form two distinct spanwise ducts. Quite separate air supplies can thus be provided to inboard and outboard nacelles, with provision for interconnection to minimise duct pressure losses when only one engine supply is required. Engine mounting positions and duct exits are provided at various spanwise stations, including the tip.

In the design and manufacture of the wings, it proved quite difficult to ensure maximum duct area whilst retaining sufficient strength to withstand the internal pressure and adequate stiffness to avoid excessive tip deflections under aerodynamic load. Careful manufacture was necessary, with heat treatment and straightening between successive stages of internal and external machining. However, with a supply pressure of 10 atmos. abs., a total flow approaching 10 lb/sec has been achieved with an adequate usable nacelle pressure of 5 atmos. abs.

As regards engine arrangements, pairs of $2\frac{1}{4}$ in. diameter simple ejector nozzles are provided, for attachment at 25%, 35% or 45% semispan, representing elementary 0° and 90° lower surface jet sources. By adding fairings, these nozzles can be converted into the corresponding ejector nacelle configurations for comparative purposes. The injector nacelles (with partial intake flow representation) and the ejector nacelles (no intake flow) can also be mounted at the same spanwise stations on pylons affording three clearances, with an alternative chordwise position at the middle clearance. The injector nacelles, with alternative intake lengths, have 0°, 30° or 90° rear nozzles of $2\frac{1}{4}$ in. diameter, and are each capable of exit velocities approaching 700 ft/sec and a thrust of some 33 lb. The ejector nacelles can be fitted with the rear nozzles, or with single lower nozzles, or with either one or two pairs of swivelling side nozzles, each configuration having a total nozzle area of 4 sq in. With the side nozzles, each ejector nacelle can produce a thrust of about 70 lb at a jet speed of about 1000 ft/sec.

For lift-engine representation, multiple injector and ejector nacelles have also been designed for attachment at 60% and 80% semispan, or at the wing tip.

4 GROUND SIMULATION BY MOVING-BELT RIG

4.1 Nature of problem

With modern high-lift systems and V/STOL aircraft, ground effects are often large and sometimes adverse. The need has arisen to check the adequacy of relevant wind-tunnel tests with the conventional fixed ground-plate since unrepresentative boundary-layer flows occur on the ground-plate. Removal of this boundary layer can be ensured by suction through the plate, but the quantity of air involved tends to be so large that extraneous 'sink' effects are superimposed on the whole flow field between the model and the simulated ground. Furthermore, the choice and control of the suction inflow distribution tends to be particularly difficult and critical over local areas where strong pressure gradients are present. Another technique requires a second 'image' model inside the tunnel working section, without an intermediate ground-plate, providing a symmetrical flow pattern above and below the free boundary. However, aerodynamic justification of this technique is difficult when appreciable ground effects are expected, particularly if strong vorticity or jet flows are present.

Again, there is a real difficulty in ensuring precise similarity in the aerodynamic behaviour of the two models under high-lift conditions. Perhaps a more natural approach to practical conditions is to eliminate the spurious relative motion between the fixed ground and the mainstream, though admittedly this is not a simple task if a satisfactory installation for research work is the aim.

An elaborate moving-belt ground rig has been developed at R.A.E.[12], essentially consisting of an 8 ft wide continuous belt, running at speeds up to 90 ft/sec over a pair of rollers of 1 ft diameter located $9\frac{1}{2}$ ft apart, installed in an $11\frac{1}{2}$ ft x $8\frac{1}{2}$ ft tunnel. The rig was designed primarily for use with existing and new models mounted on the floor virtual-centre balance, which has a special air-connector system to expedite testing of jet-blowing models on a single vertical-strut mounting. For our purposes, therefore, it was preferable to mount such models upside down in the tunnel, with the moving-belt ground above them (Fig.15). But the general description and comments which follow in Section 4.2 should apply equally well for an upright model with the ground rig below it.

An aerodynamic appraisal of essential ground test techniques, especially as regards the adequacy of the conventional fixed ground-plate approach, is in progress at R.A.E. using a wide range of models on the moving-belt rig. Some early comparisons from the experiments completed to date are mentioned in Section 4.3.

4.2 Moving-Belt Rig design

4.2.1 Structural features (Fig.16)

The metal supporting structure comprises frames in weldable aluminium, the two side frames and the bracing cross frame being bolted together. The rollers, which are 8 ft wide and made from 3/8 in. mild steel plate, rolled and machined to $\frac{1}{4}$ in. thick, are attached to a solid steel shaft (3 in. diameter) by a central as well as end fittings, to preclude shaft whirling. The amount of roller camber needed to ensure flat running of the belt against the plate proved rather smaller than anticipated, namely linear taper from a constant $12\frac{1}{2}$ in. diameter over the central 3 ft span to $12\frac{1}{4}$ in. diameter at the ends. The rollers, pitched a distance 9 ft 6 in. apart, have three of the four end bearings in longitudinal slides, each with an auxiliary motor driving a screw jack for adjustment. This permits as much as 5% extension lengthwise to ensure adequate belt tensioning, to cope with permanent elongation and to provide differential tensioning for effecting tracking control.

The main roller drive is at the fixed end-bearing, with the power supplied by a 20 h.p./400 volt A.C. motor located above the tunnel, through a manually-operated variable-speed V-belt pulley system. There is a vertical keyed shaft, a spiral bevel box (1/1 ratio), a magnetic clutch and a grooved pulley drive (1·7/1 speed increase).

The endless moving belt, made from standard 3-ply material, of overall thickness 3/16 in. and weight 32 oz/sq yd per ply, is 7 ft 10 in. wide and 22 ft long. There is a longitudinal seam because of the large width, but the

joint is staggered through the thickness of the belt; the side with a duck material facing runs adjacent to the rollers and suction plate, the normal friction surface being on the outside.

The suction box itself is made of Duralumin and comprises five compartments with 1/8 in. perforations at 3 in. pitch over the suction plate. A suction level of some 1 in. water, roughly balancing the weight of the belt, sufficed to ensure flat running; the power requirements did not become excessive, provided that suction was applied only with the belt in motion. However, even with an upright rig, some suction would seem desirable, since local negative pressures of the order 10 lb/sq ft (e.g. $C_p = -1$, $q_o = 10$) can readily occur due to aerodynamic interference effects.

A fairing 13 in. deep and overall length 15 ft 2 in. encloses the whole structure, except, of course, the flat rearward-moving belt surface for ground simulation near the model. This, as well as streamlining the rig, minimises the possibility of lift generation around the moving belt (Magnus effect). A rubbing seal on the front roller to prevent internal air circulation proved unnecessary. The nose of the fairing is symmetrical and semi-elliptic in cross-section, with suction through five rows of interrupted spanwise slits to reduce boundary-layer growth ahead of the moving belt. With the slit area of 0·013 sq ft per ft span, a depression of 4 in. water and suction flow-rate of about 1·5 lb/sec sufficed to ensure a negligible boundary-layer thickness at the rearward end of the fairing nose.

4.2.2 Calibration aspects

The belt speed is measured by direct observation to avoid errors due to belt slip or extension. An electronic timer determines the time interval for a narrow metallic mirror attached to the belt to traverse the known distance between photo-electric cell units at either end of the backing plate. Furthermore, an indication of the belt's transverse position is provided by another photo-electric device sensing a black-and-white pattern on the belt.

Naturally, the tunnel mainstream speed in that part of the divided working section containing the model (here below the belt) needs to be derived carefully, particularly since the speeds in the two parts of the working section can differ by several percent with the model in place, while the belt speed itself can cause a rise of about 1% in the speed of the relevant test section. With the model present and both the tunnel and belt running, the appropriate test air speed can be derived by subtracting the flow rate through the empty part of the working section (not containing the model) from the flow rate into the whole working section. The former follows readily from conventional pitot-static measurements, since the distribution of the velocity in the empty part is virtually unaffected by the presence of the model on the other side of the ground, while the latter follows as usual from twin rings of static pressure holes in the tunnel contraction. Of course, additional checks on both the relevant airspeed and the uniformity of distribution into the part of the working section containing the model can usefully be made by detailed explorations at the front end of the ground.

The boundary-layer characteristics actually achieved on the 'ground', with the belt moving at mainstream speed V_o, are of special importance. For example (see Fig.17), total head traverse measurements just behind the front roller position indicate a minimum airspeed V_{min} of only 0·7 V_o, at 0·1 in. from the belt surface. With the addition of suction over the nose-fairing to effect boundary-layer removal there, V_{min} increases to 0·83 V_o. Further back, corresponding to the centre of the model location, the values of V_{min} without and with nose-fairing suction are as high as 0·86 V_o and 0·93 V_o respectively, at about 0·2 in. from the belt surface. The local speed reaches the full mainstream speed at about 1·5 in. from the surface, much the same as with a fixed ground. It is worth adding that, although the boundary-layer displacement thickness there is reduced from 0·27 in. to 0·12 in. by the belt movement alone, a further reduction to 0·055 in. ensues by the addition of nose-fairing suction, and the velocity variation through the boundary layer is halved. Finally, the use of a belt speed close to the mainstream speed seems the most reasonable.

4.2.3 Future improvements

The moving-belt rig has now run reasonably well for some 120 hours, most of this under actual model test conditions. Naturally, in the light of the accrued experience, some improvements are being incorporated before the next series of model tests. Firstly, the control arrangements for belt speed, tracking and suction will be centralised, together with the appropriate visual or audio indicators, in order to facilitate coordinated control by a single operator; this now seems desirable as a safety precaution as well as for manpower economy. Secondly, a replacement belt will be fitted which has had pretensioning treatment, since permanent extensions of 2% have arisen with the old belt and even larger amounts at the centre. Furthermore, for satisfactory testing of V/STOL round jet models with choked jet exits, some modification to the central portion of the backing plate seems essential. Local jet-impingement pressures of 500 lb/sq ft or more (above ambient) on the belt generate unacceptable high friction locally, while nearby local depressions of 100 lb/sq ft or more (below ambient) cause local belt separations which could influence airflow directions under the model. Some low friction material or coating (possibly with increased suction) over the central portion of the backing plate should alleviate the problem considerably, but more sophisticated schemes are being explored. Of course, if the jet exit and associated local pressures are much reduced, say to one-half the above, no serious difficulties are likely.

4.3 Comparisons of moving and stationary ground

The R.A.E. moving-belt ground rig is first being used with a variety of model configurations, to explore whether the influence of ground proximity is influenced significantly by the extraneous boundary layer on the simple fixed ground-plate, rather than for detailed aircraft research and development with one particular configuration. Model tests have already been started on a subsonic jet-transport arrangement, a slender wing with and without body, a jet-flap wing, an air-cushion vehicle and a V/STOL jet-lift fighter configuration. For these particular types (see Fig.18), an interim appraisal will be

attempted here by comparing some force and moment measurements obtained to date. However, to be decisive, further measurements and flow studies are needed to clarify the origin of specific differences (or lack of them) due to moving ground, with any peculiarities of the particular model in mind. The relative size of models to tunnel has been kept reasonably small, to minimise any effects due to possible changes in tunnel constraint and blockage corrections with belt movement.

4.3.1 Subsonic jet-transport configuration (Fig.19)

The model configuration chosen as representative of a subsonic civil jet-transport configuration had an aspect-ratio 7 wing of 5 ft span, with 10% thickness-chord ratio, 33° quarter-chord sweep-back, a large-span L.E. slat, and an inboard T.E. flap deflected 20°. Typically[13], for a ground clearance $h = 0{\cdot}7\bar{c}$, the improved simulation by belt movement leads to some alleviation of the fall-off in lift-incidence curve slope experienced before the stall (due to ground constraint) together with a slight increment $\delta C_{Lmax} = 0{\cdot}07$ in maximum lift coefficient; but this is not large compared with the basic change $\Delta C_{Lmax} \simeq -0{\cdot}3$ from ground effect (belt stationary). Again, just below the stall, the belt movement gives only small reduction $\delta C_D \simeq -0{\cdot}01$ in drag at a prescribed lift coefficient, compared with the basic change $\Delta C_D \simeq -0{\cdot}05$. The change in moment coefficient due to belt movement is also not large, tending to reduce the magnitude of the increments due to ground both tail-off and tail-on. For the plain-wing configuration (high-lift devices retracted), the lift, drag and moment changes due to belt movement were practically negligible.

In assessing these results, it should be noted that the directly comparative tests have, for rig reasons, to be made at an airspeed not much above 80 ft/sec rather than the full-scale speed of 200 ft/sec, while the model is only about 1/25th full-scale. In fact, the lift and drag changes due to belt movement are the same order of magnitude as those resulting from doubling the test speed and Reynolds numbers, with the belt stationary. Broadly speaking, it seems reasonable to assume that the use of the conventional fixed ground-plate only slightly exaggerates the changes due to ground effect for subsonic jet-transport configurations, at least with high-lift devices giving moderate C_{Lmax} values ($\simeq 2{\cdot}5$) away from ground.

4.3.2 Slender wing (Fig.20)

The slender wing model had an aspect-ratio 1·36 gothic planform of 3 ft span, with a sharp leading-edge swept back 70°; tests were made without and with a long body of circular cross-section[14]. For the wing without body at the smallest ground clearance $h = 0{\cdot}13c_o$ of the pivot point ($x = 0{\cdot}57c_o$), the belt movement leads to some increase in lift at the higher incidences, e.g. $\delta C_L \simeq 0{\cdot}05$ near $\alpha = 15°$, but this is small compared with the basic gain $\Delta C_L \simeq 0{\cdot}3$ from ground effect (belt fixed). The corresponding changes in moment and drag coefficients due to belt movement are insignificant when comparison is made at the same lift coefficient. In fact, detailed pressure-plotting studies on the wing show that the belt movement causes a general change in the surface pressure

distribution rather than alleviations concentrated at the trailing edge, even at $\alpha = 15°$ where the trailing edge is nearly touching the ground, while upper and lower surface changes are of the same order of magnitude. Similar arguments hold even when the body is added.

Thus, it again seems reasonable to accept the conventional fixed ground-plate for tests on slender wing models, at least unless special high-lift or jet-deflection devices are under consideration.

4.3.3 Jet-flap wing (Fig.21)

The nature and magnitude of the effects of ground proximity for jet-flap wings were previously investigated by detailed experiments on the R.A.E. jet-flap complete model with a fixed ground-plate[15], but it was fully appreciated that unrepresentative effects could occur from interactions between the jet sheet (or entrained flow) and the ground-plate boundary layer. This model has therefore been extensively re-tested on the moving-belt rig[16]. The aspect ratio 9 wing, of 6 ft span, has a highly-cambered thick section (NACA 4424), with an 11% chord T.E. flap (full-span except for the body cut-out); a thin jet sheet is ejected from a slit in the flap shroud and clings to the upper surface of the deflected flap. The strut entry into the fuselage upper surface, with the high-wing position, necessitated the addition of local auxiliary B.L.C. to minimise flow separations on the model surface near the junction. Because of this and other model changes, the results quoted with the belt stationary should not be compared directly with those obtained previously with the fixed ground-plate.

Some typical measurements of lift, moment, thrust and downwash (high tail) are shown in Fig.21, without and with belt movement at mainstream speed, with a jet deflection angle $\theta = 50°$ and a ground clearance $h = 1{\cdot}5\bar{c}$ for the wing. Except for downwash, no significant changes from belt movement arise until the jet momentum coefficient $C\mu$ or the jet angle to the mainstream $(\alpha + \theta)$ are large enough to cause jet impingement on the ground. Then, belt movement produces some recovery of lift-incidence slope before the stall, stalling incidence and C_{Lmax}, with accompanying increases in nose-down pitching moment (tail-off), thrust and downwash. For example, with $C\mu = 4$ and $\theta = 50°$, the lift increment due to belt movement $\delta C_L = 0{\cdot}7 \pm 0{\cdot}1\ C_L$ at $\alpha \simeq 15°$, the stalling incidence with the belt stationary. Moreover, detailed flow studies imply that the incidence at which a significant part of the jet begins to flow upstream along the ground can be delayed as much as 10° by the belt movement, with associated increases in circulation and stalling incidence.

Thus, the conventional fixed ground appears to exaggerate the influence of ground proximity significantly only under conditions of severe jet impingement, when large ground effects are, in fact, present.

4.3.4 Air-cushion vehicle (Fig.22)

The performance of air-cushion vehicle models in a mainstream might reasonably be expected to be seriously affected by the presence of the ground-plate boundary layer. The model tested on the moving-belt ground[17] is representative of the Britten-Norman C.C.2 arrangement, with a near-rectangular planform

5 ft long and 3 ft wide, and twin Heba fans (centrifugal-type) feeding a peripheral slot on the underside of the vehicle. For a ground clearance $h = 2{\cdot}7$ in. ($= 0{\cdot}05\sqrt{4S/\pi}$), at zero incidence and constant fan r.p.m., the belt movement leads to negligible changes in the critical speed at which the mainstream dynamic head reaches the static cushion pressure, when the air-cushion is first penetrated by the mainstream. Furthermore, there are no noticeable changes in lift and drag, up to the critical speed at least, though the nose-up moments are reduced by nearly one-third in the neighbourhood of the critical speed. In fact, the lower surface pressures on the model are affected far more by mainstream speed variation than by belt movement.

Unfortunately, the generalisation of results from such models is not straightforward, particularly when the jet dynamic head is low (here 5 lb/sq ft), since the peripheral distribution of exit momentum varies appreciably with mainstream speed, incidence and belt speed, with associated interaction on the fan and duct flows. Hence, at this stage, the present comparisons, though encouraging, cannot be assumed to be valid for air-cushion vehicles in general.

4.3.5 Jet-lift configuration (Fig.23)

Jet impingement and entrainment effects lead to local areas of high pressure and low pressure on the ground with jet-lift configurations, so that the associated flow patterns around the wing and body might well be modified significantly at low mainstream speeds by jet interaction with the boundary layer on a fixed ground-plate. One jet-lift model, with four exits in the body and a high wing configuration, has been tested on the moving-belt rig[7]; but only briefly because of running problems associated with permanent belt extension and local belt separation from the present backing plate, as already mentioned in Section 4.2.3. For a wing ground clearance $h = 0{\cdot}55\sqrt{4S/\pi}$, a jet thrust loading $T/S = 55$ lb/sq ft and jet angles $\theta_J = 90°$, belt movement seems to have little effect on lift or moment (tail-off), even though the impact pattern of the jets on the belt and corresponding upflow over the model change considerably with mainstream speed and incidence.

Naturally, these results envisage acceptance of the fixed ground-plate as adequate for such model, but further checks are necessary over a wide range of jet angles and forward-speed ratios, while tailplane contributions must also be studied.

4.4 Provisional conclusions on aerodynamic needs

For conventional aircraft configurations with high-lift mechanical flaps, and for slender delta-wing arrangements, there seems to be no justification for further moving-belt ground tests. Indeed, it seems preferable to rely on the results from tests with the conventional fixed ground-plate at higher Reynolds numbers than feasible with the moving ground in practice, accepting that there may be some slight exaggeration of ground effects due to the extraneous boundary-layer on the ground-plate.

With jet-flap configurations, the effect of the ground-plate boundary layer appears to be significant only under conditions of jet-sheet impingement, when further studies at larger jet angles and lower wing heights from the ground than in Section 4.3.3 would merit consideration with practical $C\mu$-values. The influence of the mainstream-speed/jet-speed ratio on the boundary layer interaction for a prescribed $C\mu$-value (varying jet sheet thickness) also warrants examination.

The present evidence with one specific peripheral-jet model arrangement on the moving ground cannot be generalised without qualification to other air-cushion vehicle models. Some further tests are therefore planned, including detailed studies on a pure jet-blowing model with the exit flow distribution carefully controlled and measured.

Although for fuselage round-jet arrangements, the effect of the ground-plate boundary layer promises to be small, further moving ground investigations are needed to cover a wider range of jet angles, mainstream-speed/jet-speed ratios, and ground clearances, particularly as regards the influence on the flow field in the vicinity of the tailplane. For jet-lift subsonic transport arrangements with lift/thrust or pure lift engines in nacelles on the wings, the results and conclusions may well be quite different, so experiments are planned on such a model.

Overall, aerodynamic measurements with a fixed ground-plate are already justified over a much wider range than could have reasonably been expected. Except in the extreme case mentioned above, the presence of the extraneous boundary layer seems to exaggerate ground effects only slightly. Moreover, there is now reasonable hope that our further researches will confirm that the moving-belt ground installation may only be needed in the future for a few special investigations or limited checks and control tests. In these circumstances, the main body of testing could then continue to be carried out using the conventional fixed ground-plate, with resulting advantages in simplicity of rigging, ease of testing, and maximum test speed.

5 ACKNOWLEDGMENTS

The authors have made use of the experience and test results of several members of the Low-Speed Tunnels Division at R.A.E. (Farnborough and Bedford) in the preparation of this paper. Particular mention should be made of specific contributions from M.N. Wood and L.A. Wyatt towards Sections 3.3 and 3.4 respectively.

Some of the models were designed and constructed by British firms in conjunction with the R.A.E.

REFERENCES

No.	Author	Title, etc.
1	Williams, J. Butler, S.F.J.	Experimental methods for testing high lift B.L.C. and circulation control models. Boundary-layer and flow control, Vol.1, pp.390 to 423. Pergamon Press. London (1961).
2	Anscombe, A. Williams, J.	Some comments on high-lift testing in wind-tunnels with particular reference to jet-blowing models. R.Ae.Soc., Vol.61, pp.529 to 540 (1957).
3	Butler, S.F.J. Williams, J.	Further comments on high-lift testing in wind-tunnels with particular reference to jet-blowing models. Aero Quart., Vol.XI, pp.285 to 308 (1960).
4	Trebble, W.J.G.	Wind-tunnel experiments on a simple lifting-jet body with and without wings. R.A.E. Tech. Note Aero 2882. (1963).
5	Eyre, R.C.W.	Description of model and test rig for flap blowing tests with slipstream in the 24 ft wind-tunnel. R.A.E. Tech. Note Aero 2919. (1963).
6	Butler, S.F.J. Williams, J.	Three-component force measurements and flow visualisation on a simple multi-jet rectangular wing model. R.A.E. unpublished paper.
7	Wood, M.N.	Data from R.A.E. tunnel tests on some fuselage-jet V/STOL configurations.
8	Wood, M.N.	Low-speed tunnel tests of a 1/10th-scale model of the Hawker P.1127 V/TOL strike aircraft. R.A.E. unpublished paper.
9	Wood, M.N. Howard, J.B.W.	The development of injector units for jet-lift engines simulation on low-speed tunnel models. R.A.E. Tech. Note to be issued. (1964).
10	Wyatt, L.A.	Preliminary note on wind-tunnel tests of a wing fitted with multiple lifting fans. R.A.E. Tech. Note Aero 2643. (1959).
11	Trebble, W.J.G. Williams, J.	Exploratory wind-tunnel investigations of a bluff body containing a lifting fan. R.A.E. Tech. Note Aero 2754. A.R.C. Current Paper No.597. (1961).
12	Butler, S.F.J. Moy, B. Pound, T.	A moving-belt rig for ground simulation in low-speed wind-tunnels. R.A.E. Tech. Note Aero 2937. (1963).

REFERENCES (CONTD)

No.	Author	Title, etc.
13	Butler, S.F.J. Eyre, R.C.W.	Data from R.A.E. tunnel tests on a subsonic jet-transport model.
14	Kirby, D.A.	Data from R.A.E. tunnel tests on two slender-wing models.
15	Butler, S.F.J. Guyett, M.B. Moy, B.A.	Six-component low-speed tunnel-tests of jet-flap complete models, with variation of aspect-ratio, dihedral and sweepback, including the influence of ground proximity. R.A.E. Report No. Aero 2652. (1961).
16	Butler, S.F.J. Moy, B.A. Hutchins, G.D.	Low-speed tunnel tests of an aspect-ratio 9 jet-flap complete model with ground simulation by moving-belt rig. R.A.E. Tech. Note to be issued. (1964).
17	Trebble, W.J.G.	Data from R.A.E. tunnel tests on an air-cushion vehicle model (C.C.2).
18	Williams, J.	(a) Some British research on the basic aerodynamics of powered lift systems. J.Roy.Ae.Soc., Vol.64, pp.413 to 437. (1960). (b) Comments on some recent research on V/STOL aerodynamics. AGARD Fluid Mechanics Panel Meeting, Paris, July 1962.

Attached:

Drg. Nos. 45125s - 45143s
Neg. Nos. 165,324 - 165,330
Detachable Abstract Cards

ADVANCE DISTRIBUTION:

DGSR(A)
DCA(RD)
ADAR
ADSR(A)
NGTE
NPL (Aero Div)
TIL - 240
Secretary, ARC

45125 S

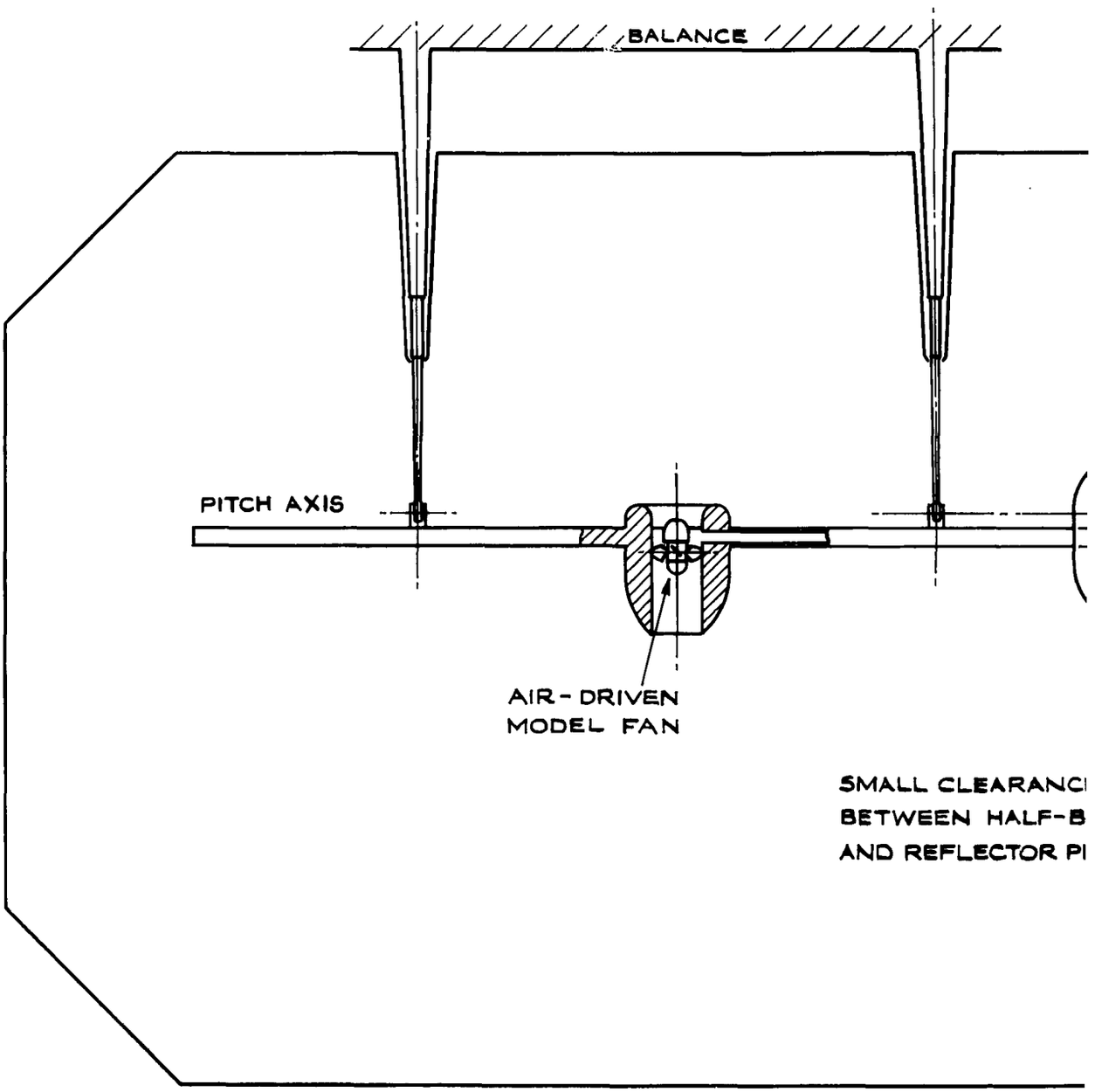

1

FIG. 1. R.A.E. HALF-MODEL CONVENTIONAL-BAL

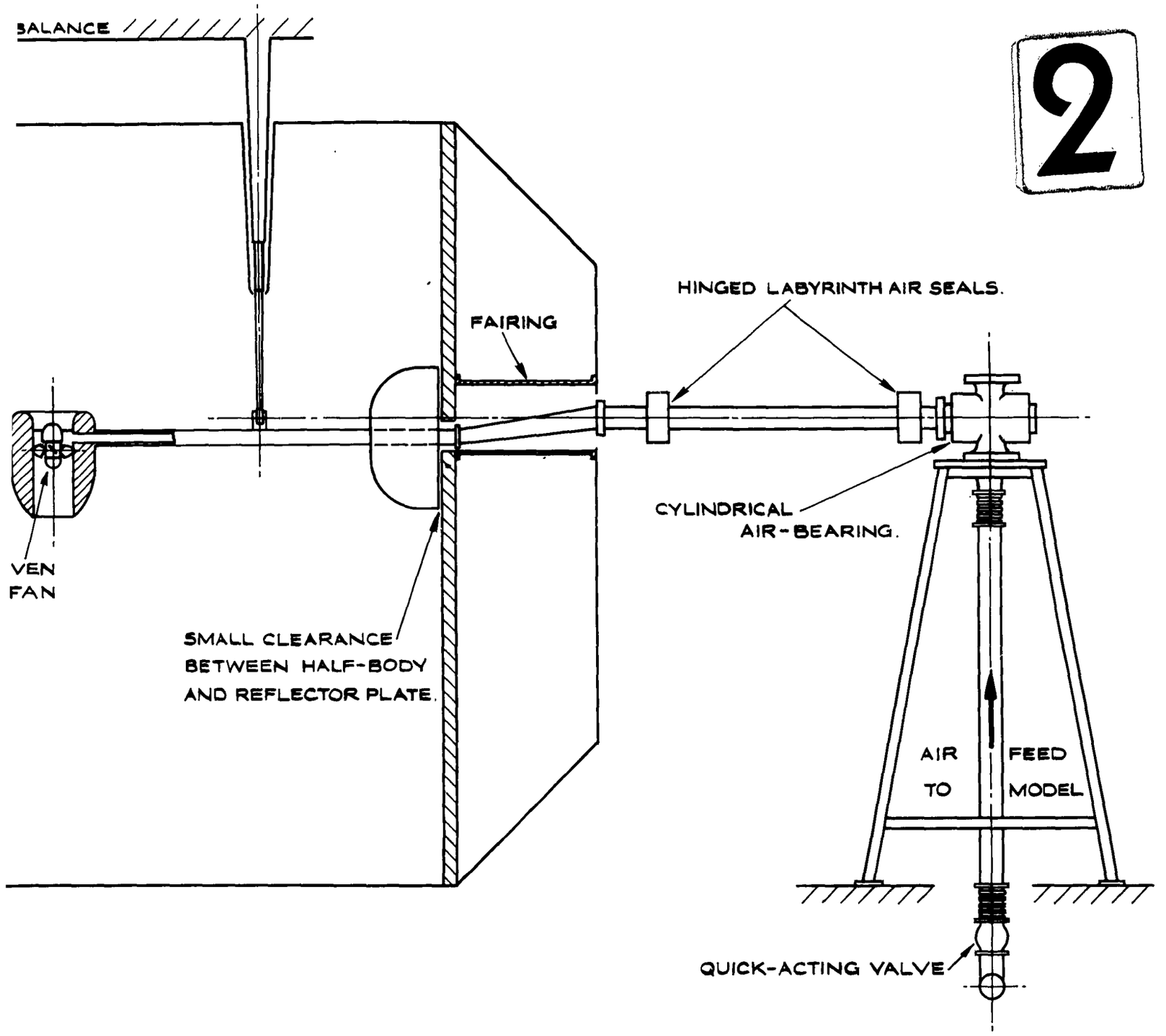

MODEL CONVENTIONAL-BALANCE RIG WITH AIR CONNECTORS.

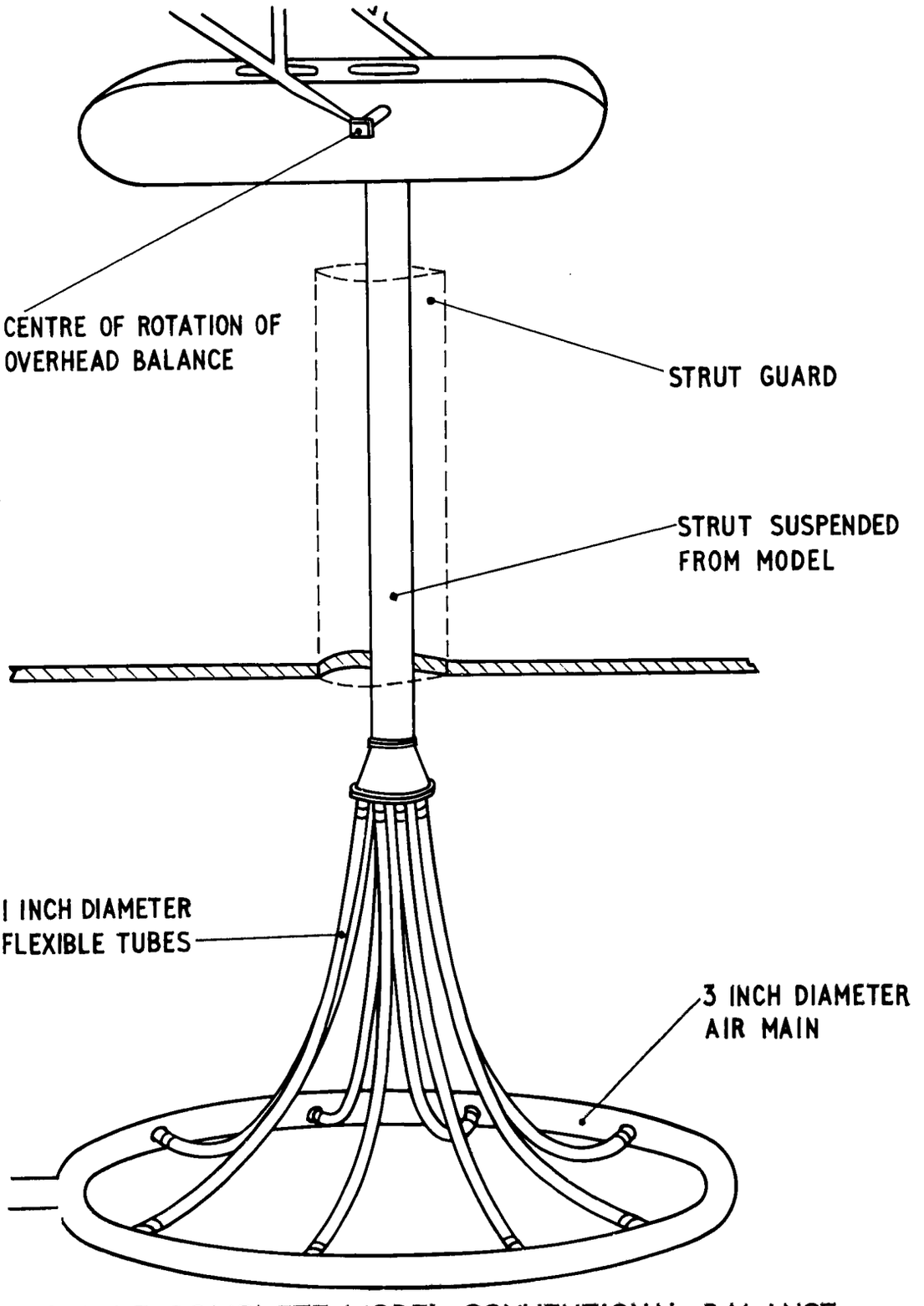

FIG.2 R.A.E. COMPLETE-MODEL CONVENTIONAL-BALANCE RIG WITH SIMPLE FLEXIBLE CONNECTORS.

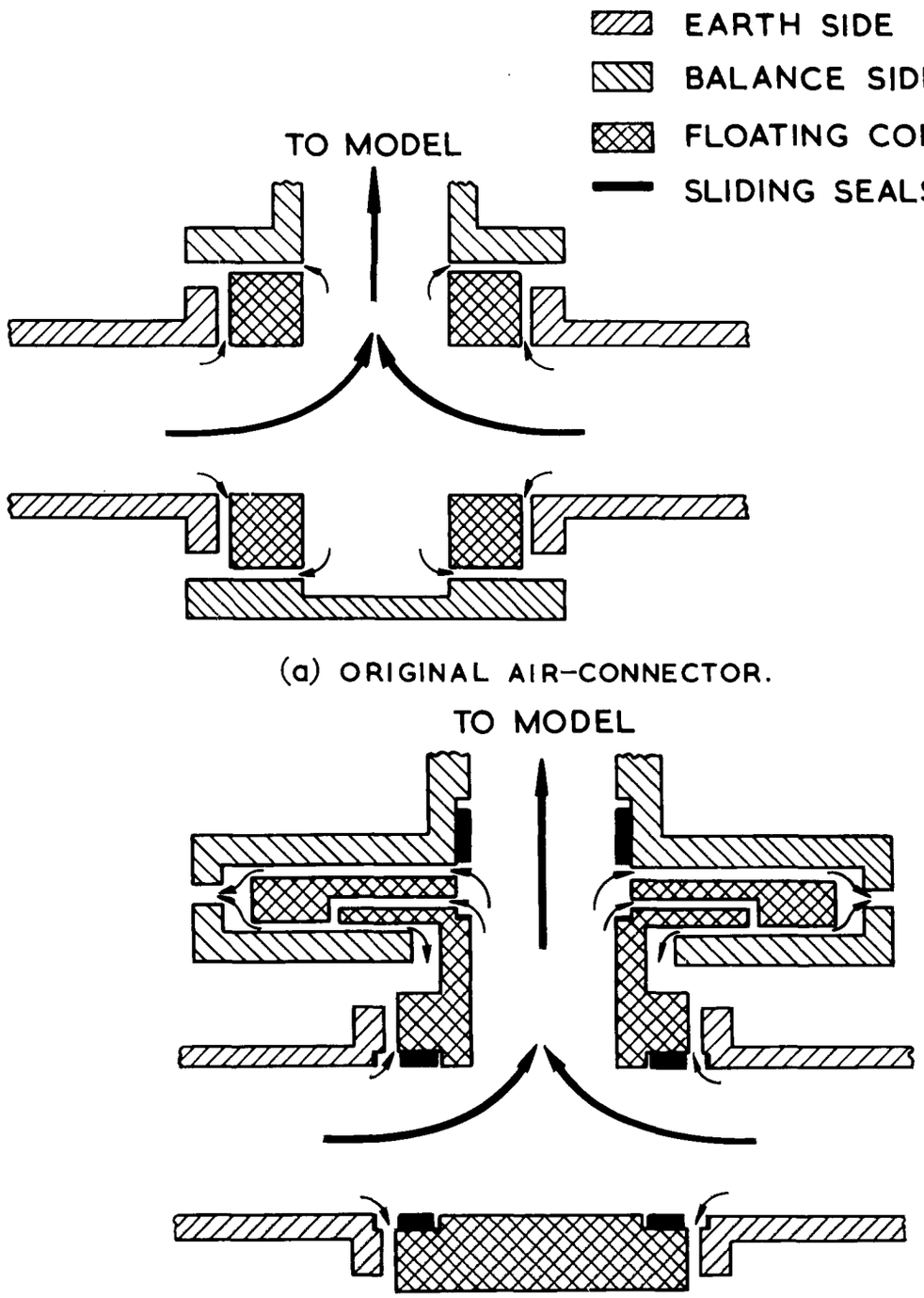

(a) ORIGINAL AIR-CONNECTOR.

(b) IMPROVED AIR-CONNECTOR.

FIG. 3. AIR — BEARING CONNECTORS FOR R.A.E. VIRTUAL-CENTRE BALANCE RIG.

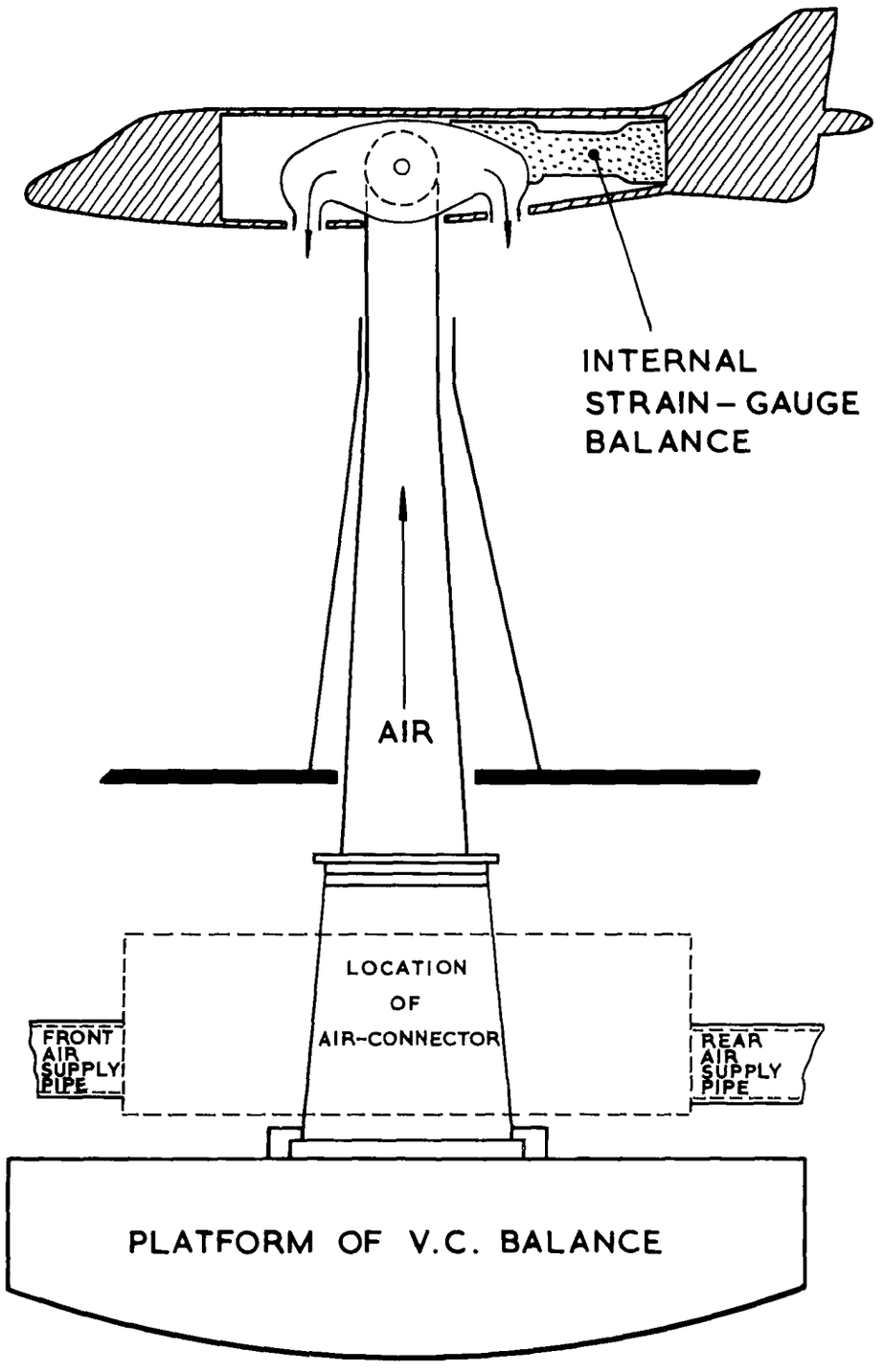

FIG. 4. COMPOSITE-MODEL RIG FOR R. A. E. VIRTUAL-CENTRE BALANCE.

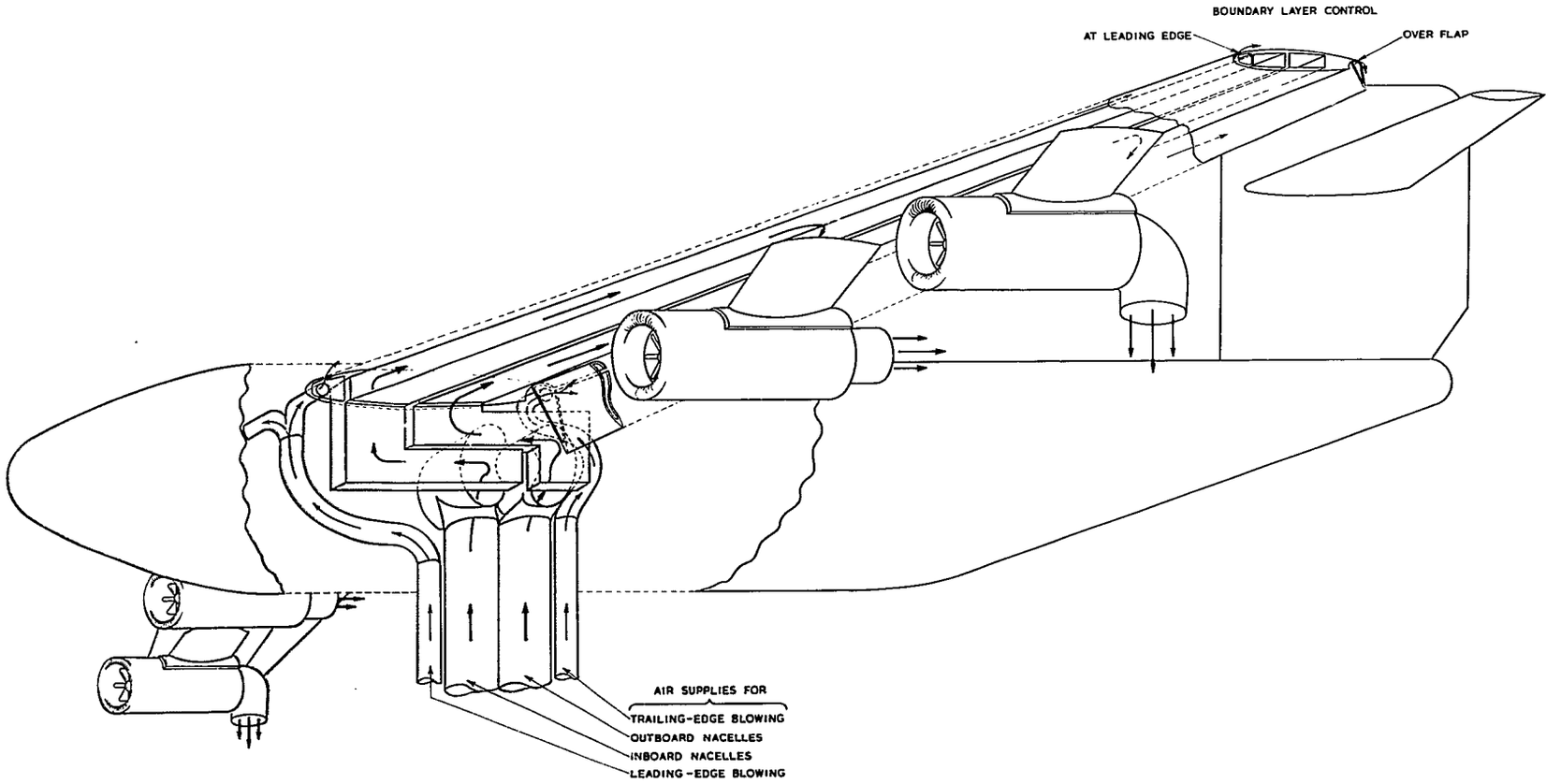

(a) GENERAL MODEL ARRANGEMENT

FIG. 5. R. A. E. SUBSONIC-TRANSPORT JET-NACELLE RESEARCH MODEL.

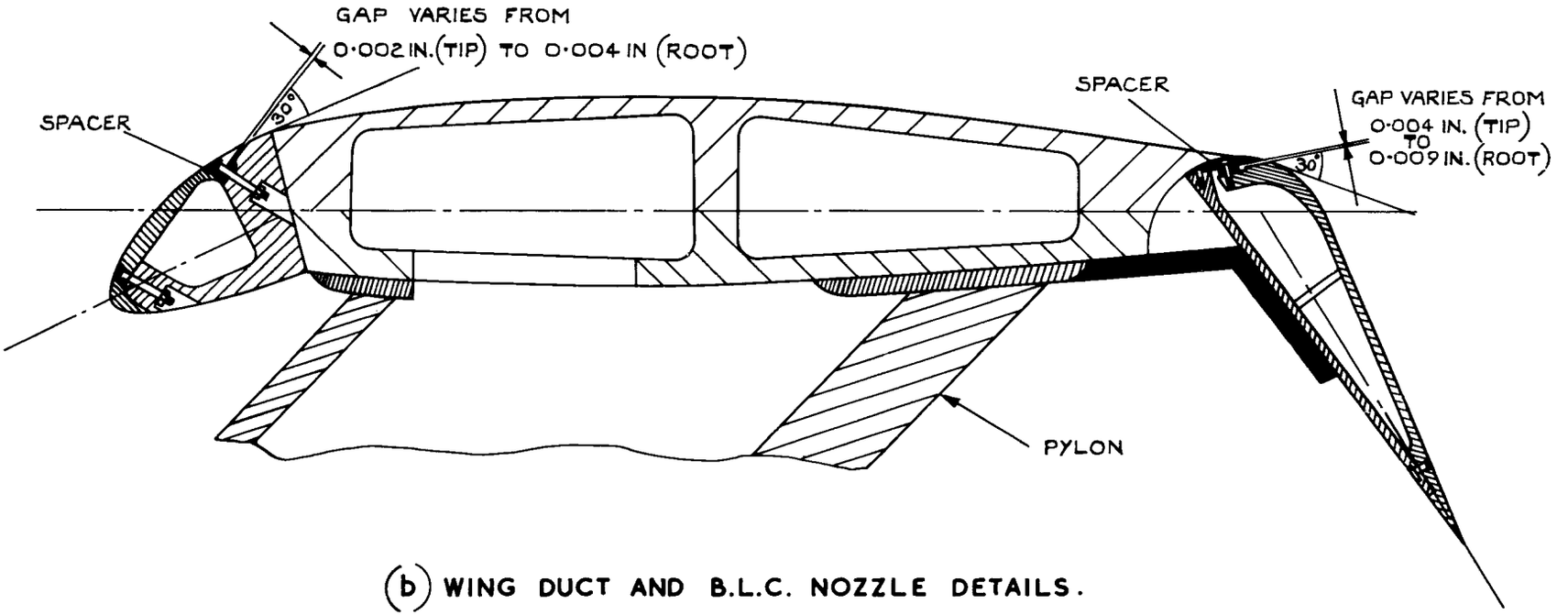

(b) WING DUCT AND B.L.C. NOZZLE DETAILS.

T.N. AERO 2944.
FIG.5(b).

FIG.5.(CONT'D.) R.A.E. SUBSONIC - TRANSPORT JET - NACELLE RESEARCH MODEL.

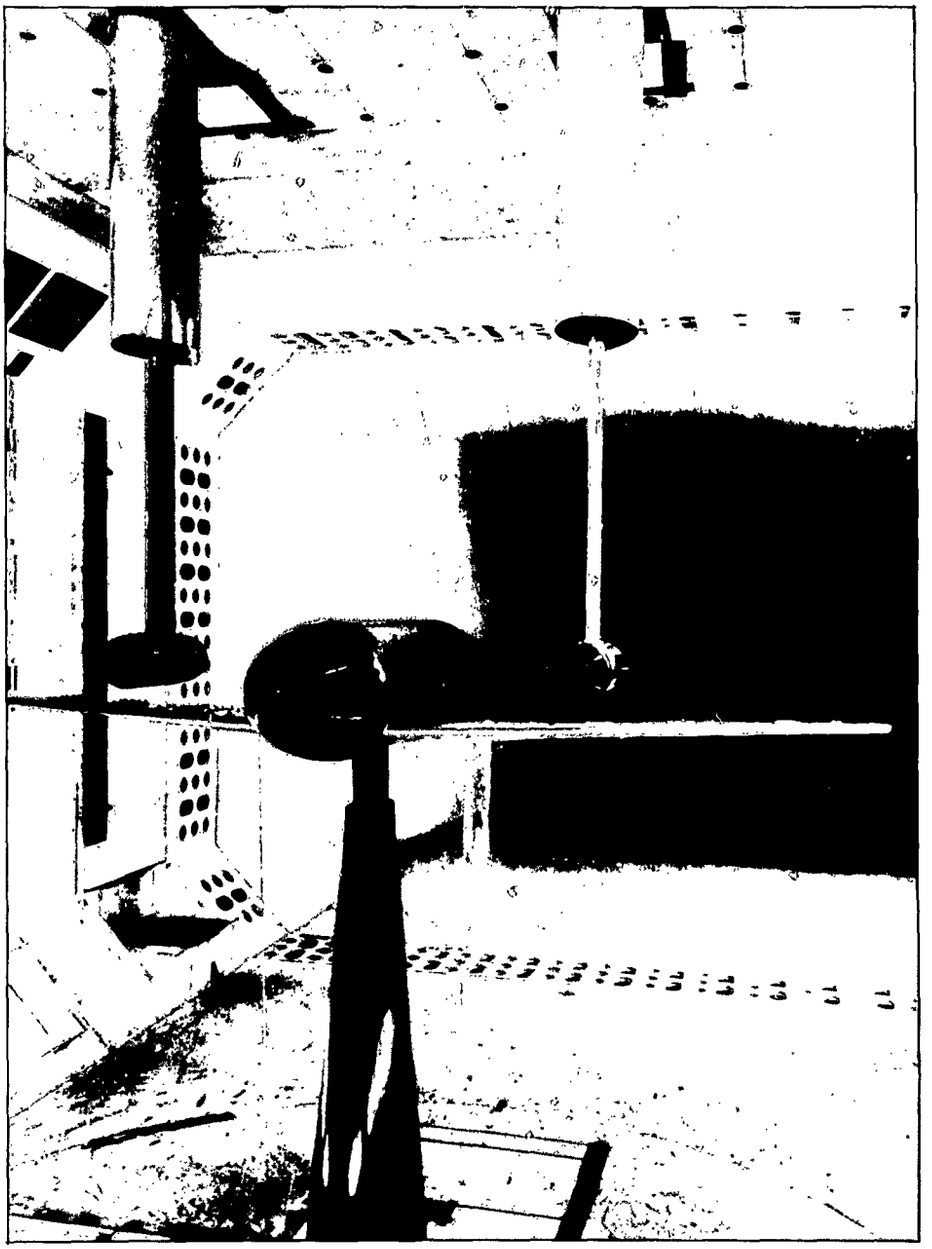

FIG.6. COMPOSITE-MODEL RIG FOR JET-NACELLE MODEL

R.A.E: 165324 64

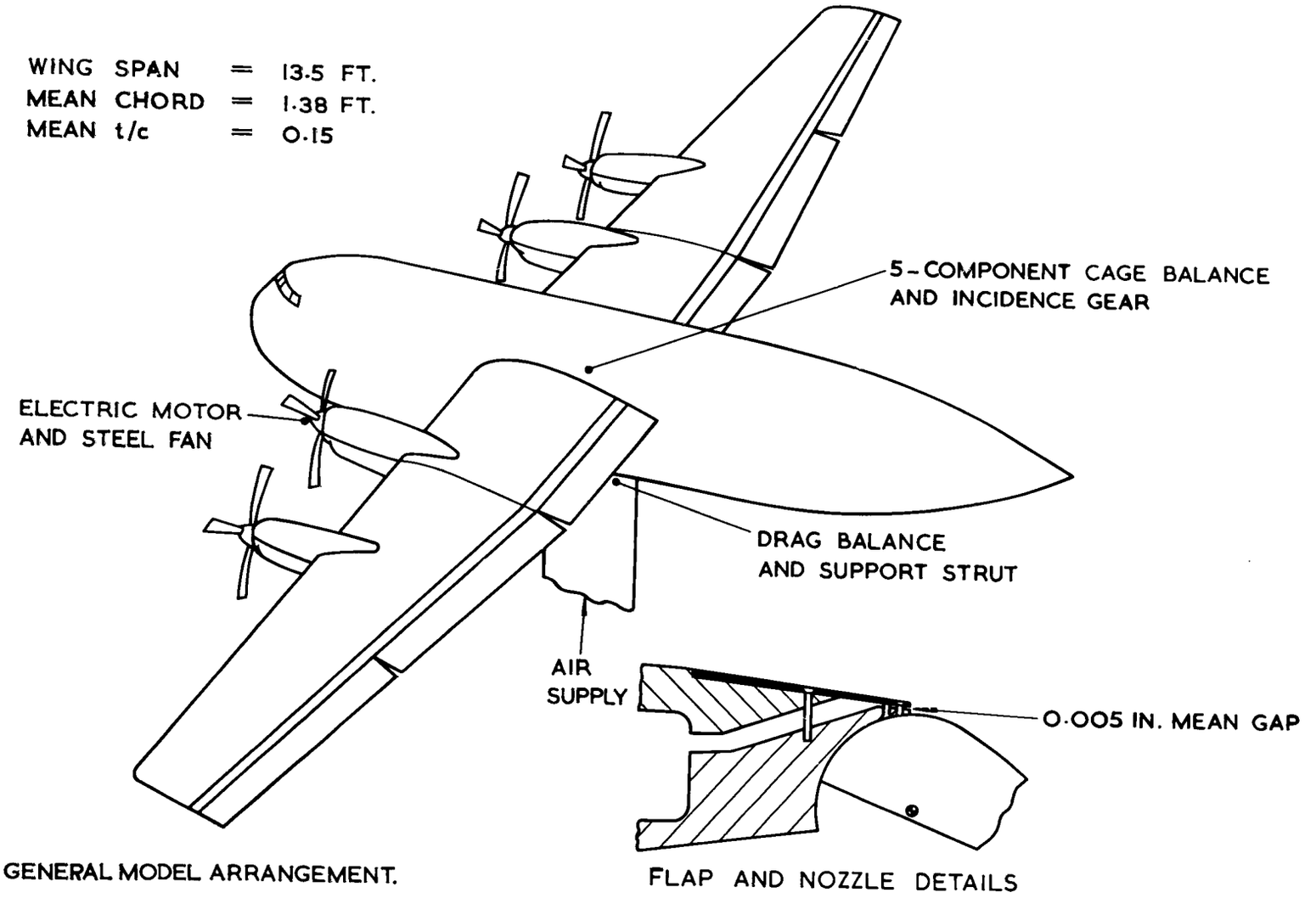

FIG. 7. ASPECT-RATIO 10 MODEL WITH TRAILING-EDGE FLAP BLOWING & PROPELLER SLIPSTREAM.

T. N. AERO. 2944.

FIG. 7(a).

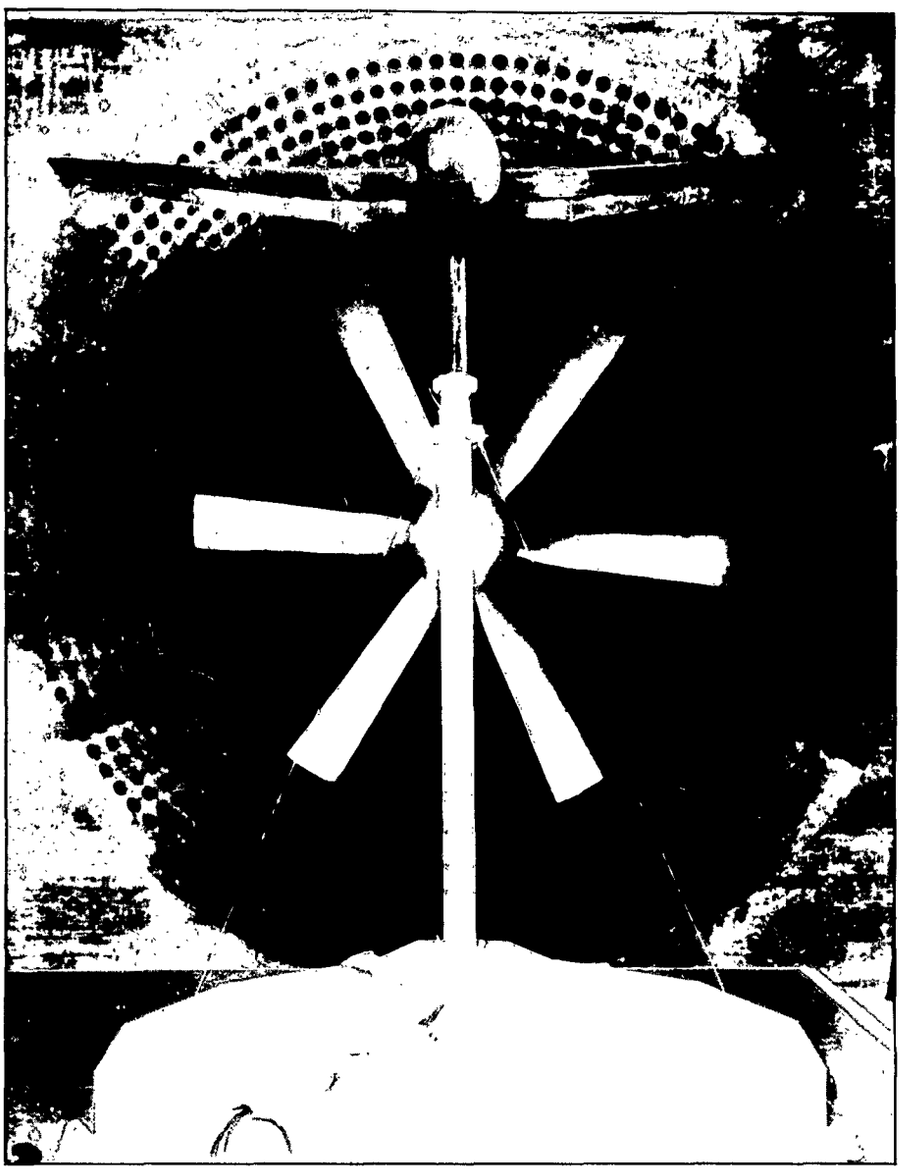

(b) 24FT TUNNEL RIG

FIG.7.(Contd.) ASPECT-RATIO 10 MODEL WITH TRAILING-EDGE FLAP BLOWING AND PROPELLER SLIPSTREAM

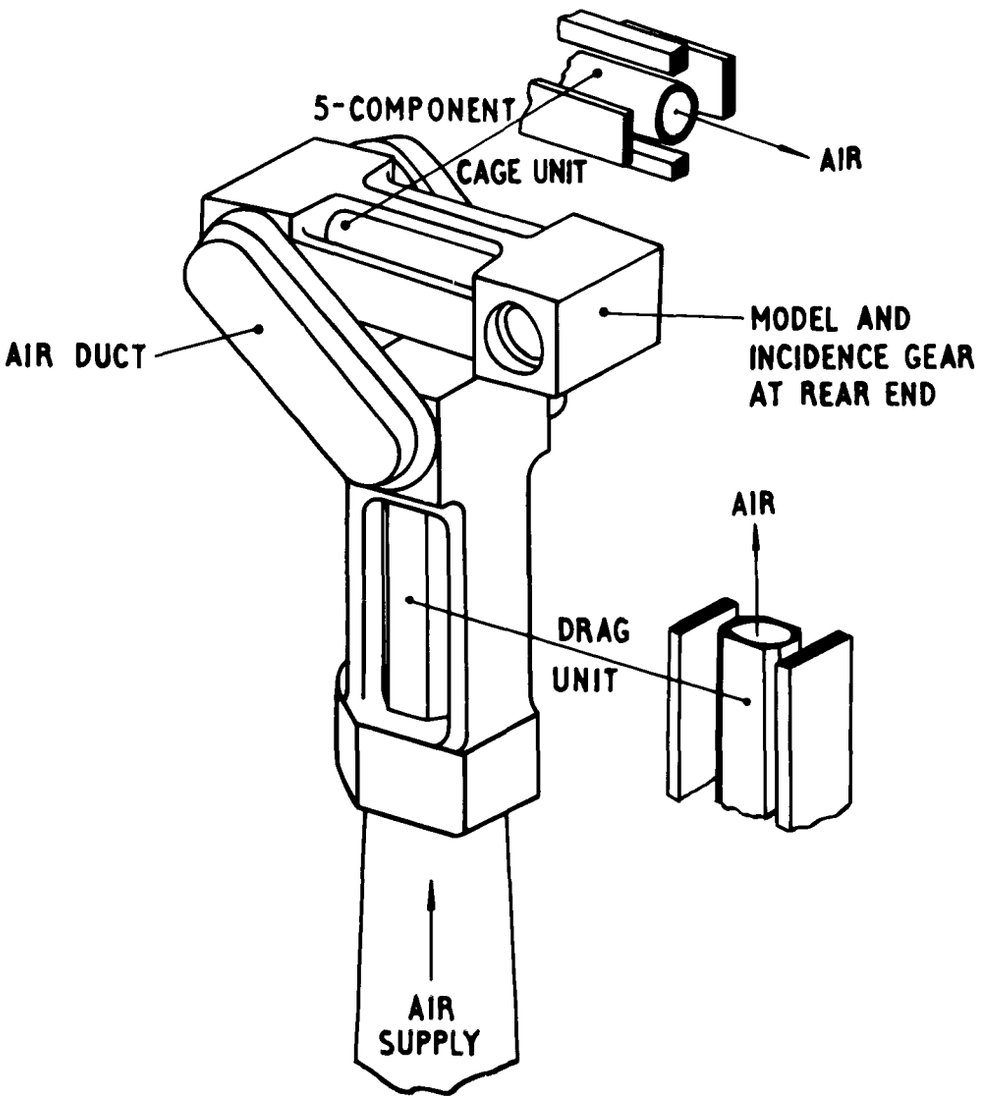

FIG.8. SIX-COMPONENT STRAIN-GAUGE BALANCE FOR ASPECT-RATIO 10 MODEL WITH TRAILING-EDGE FLAP BLOWING.

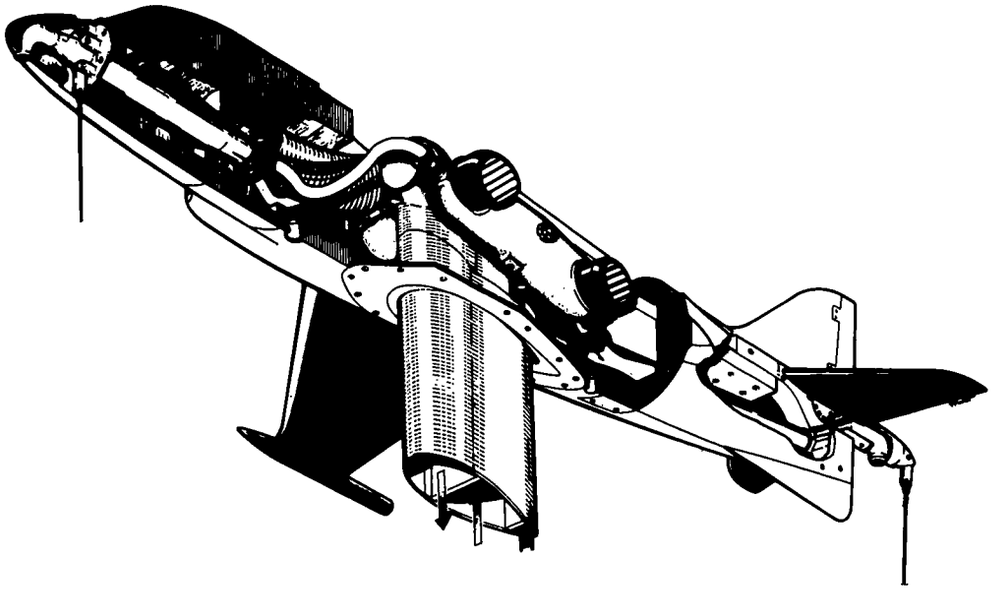

(a) GENERAL MODEL ARRANGEMENT

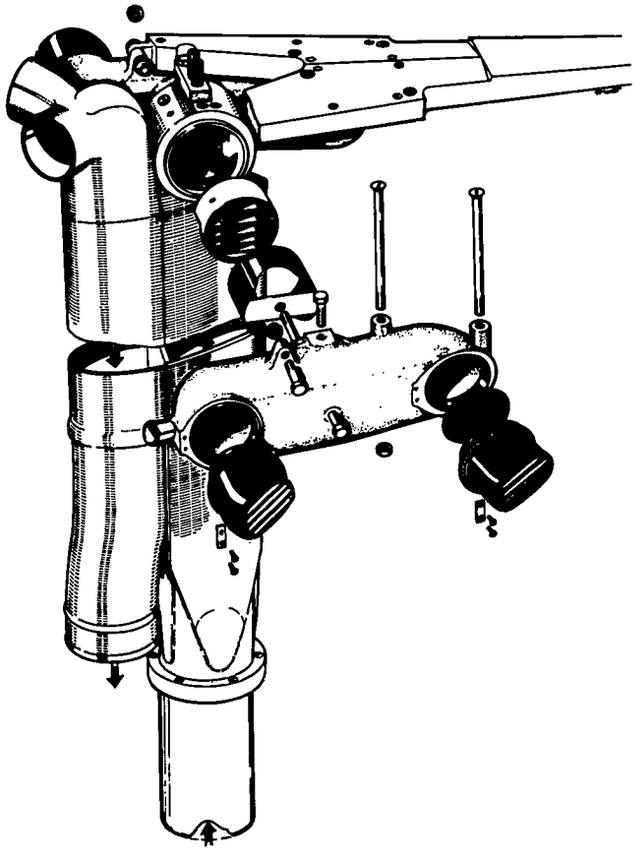

(b) DUCTING AND NOZZLE DETAILS

FIG.9. HAWKER P.1127, 1/10th SCALE MODEL

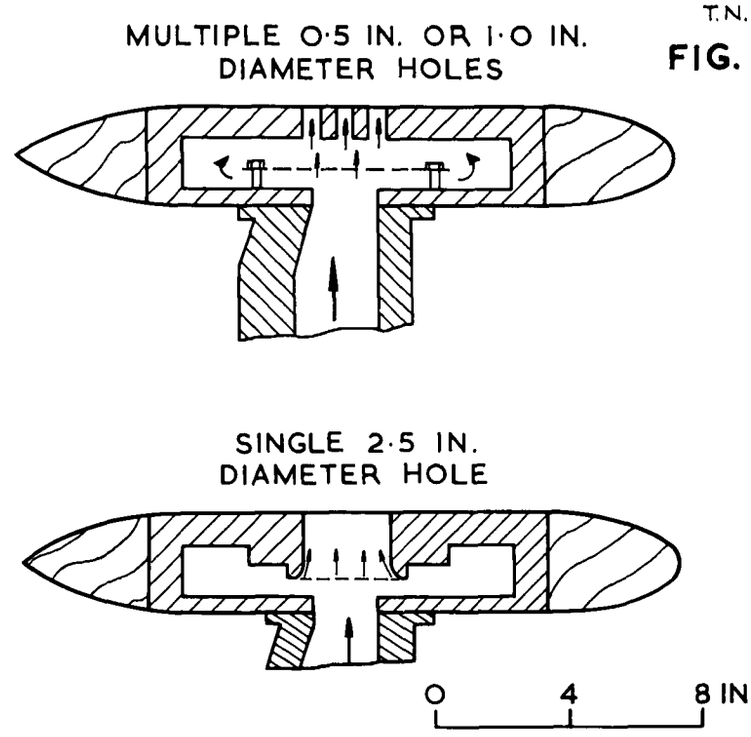

(a) SIMPLE WING–JET MODEL.

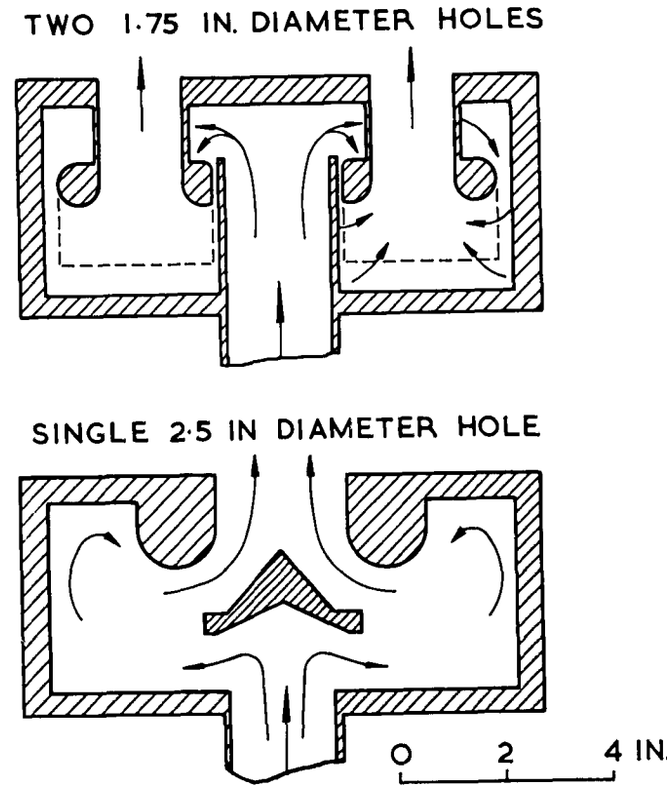

(b) SIMPLE FUSELAGE–JET MODEL.

FIG. 10. PRESSURE CHAMBER AND NOZZLE DETAILS FOR ELEMENTARY JET-LIFT MODELS.

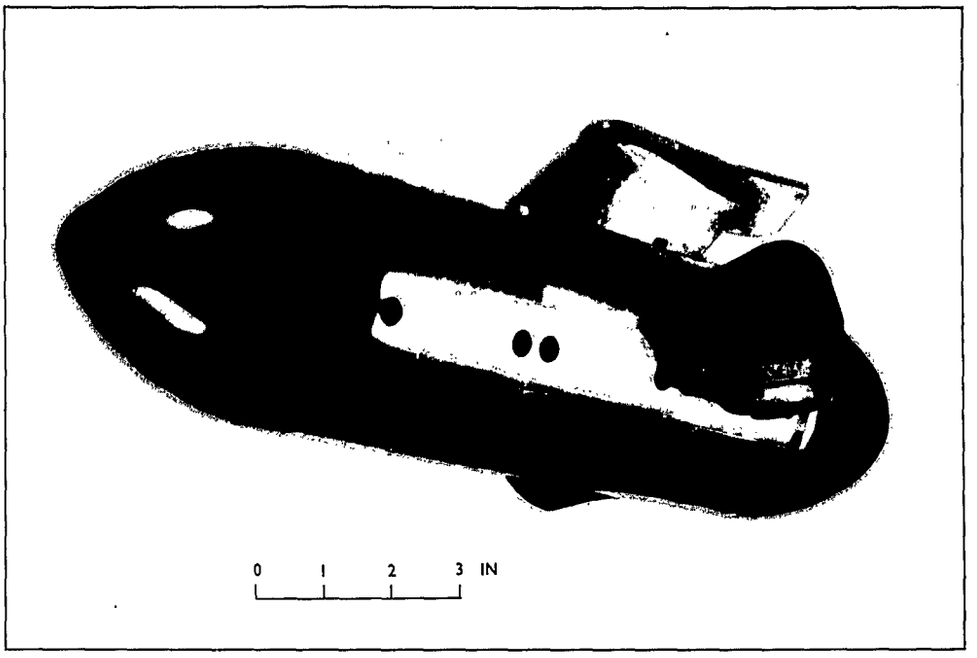

(a) GENERAL VIEW

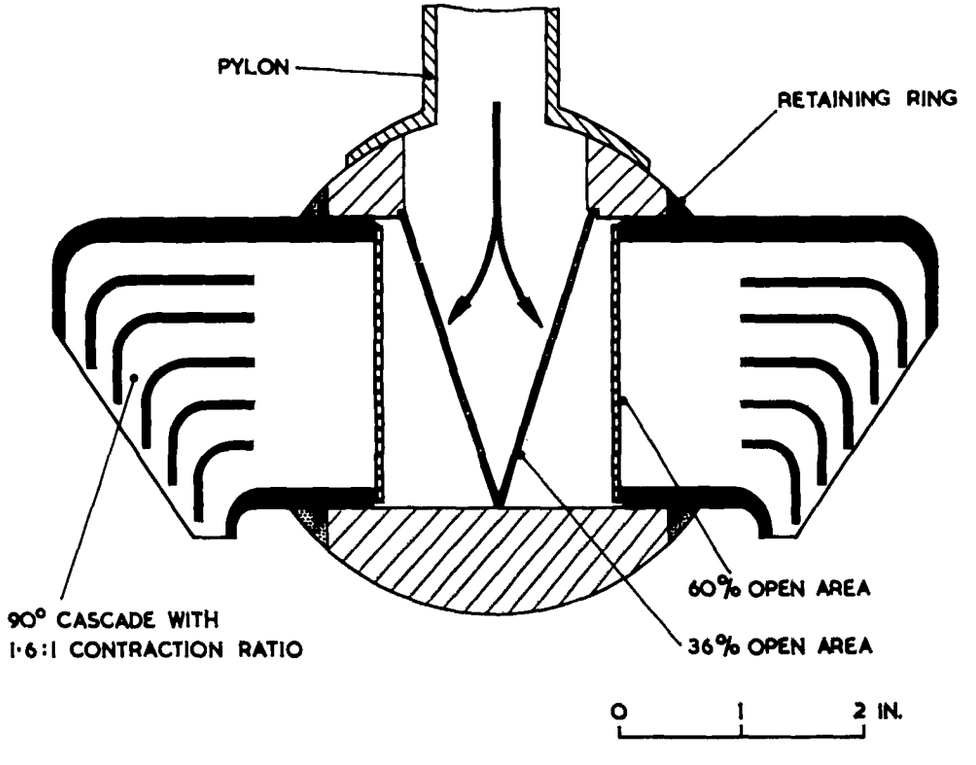

(b) PRESSURE CHAMBER AND NOZZLE DETAILS

FIG.11. TYPICAL EJECTOR NACELLE FOR JET-EFFLUX SIMULATION

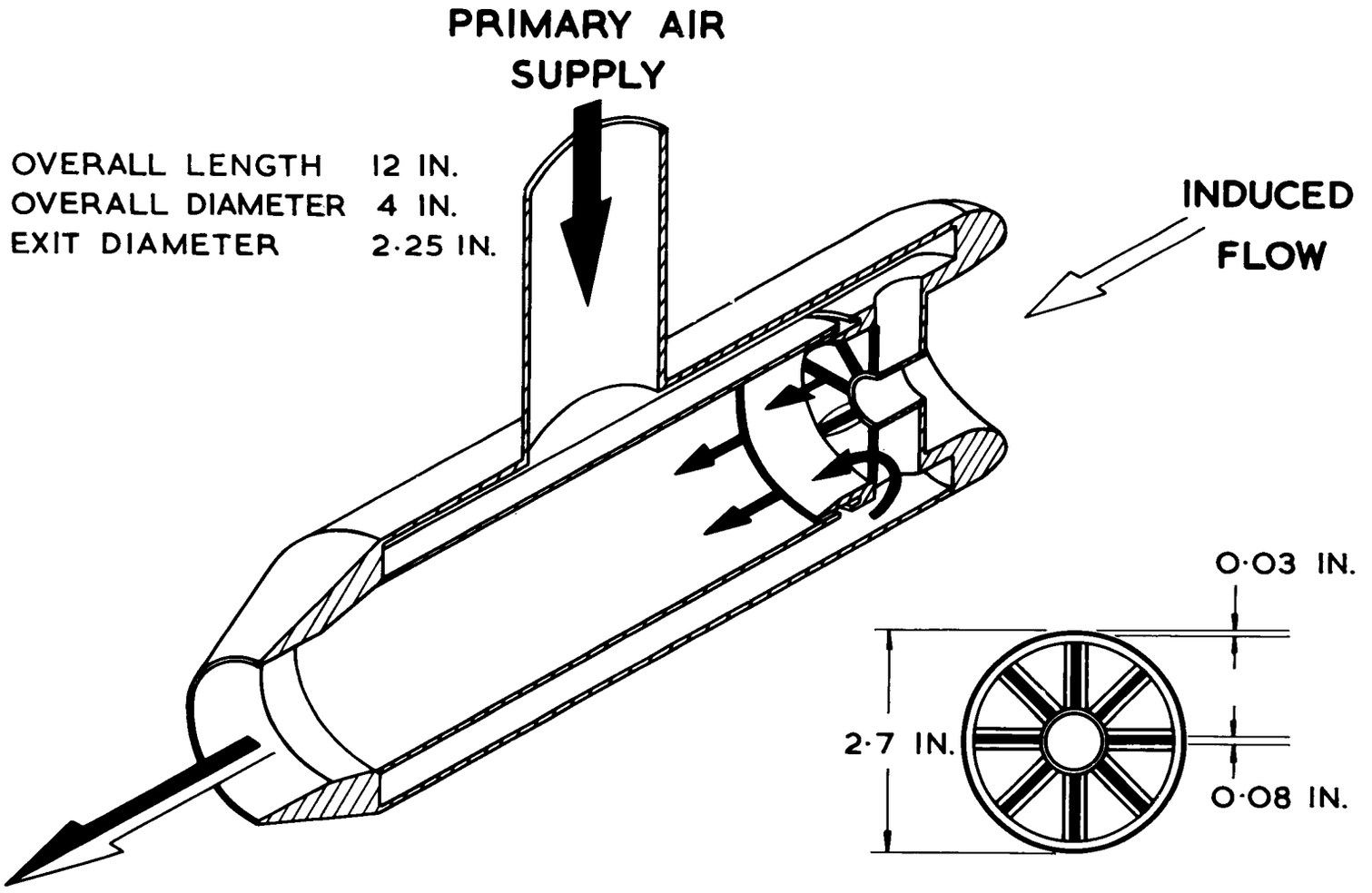

FIG. 12. TYPICAL INJECTOR NACELLE FOR JET–EFFLUX AND INTAKE–FLOW SIMULATION.

T.N. AERO 2944.
FIG. 12.

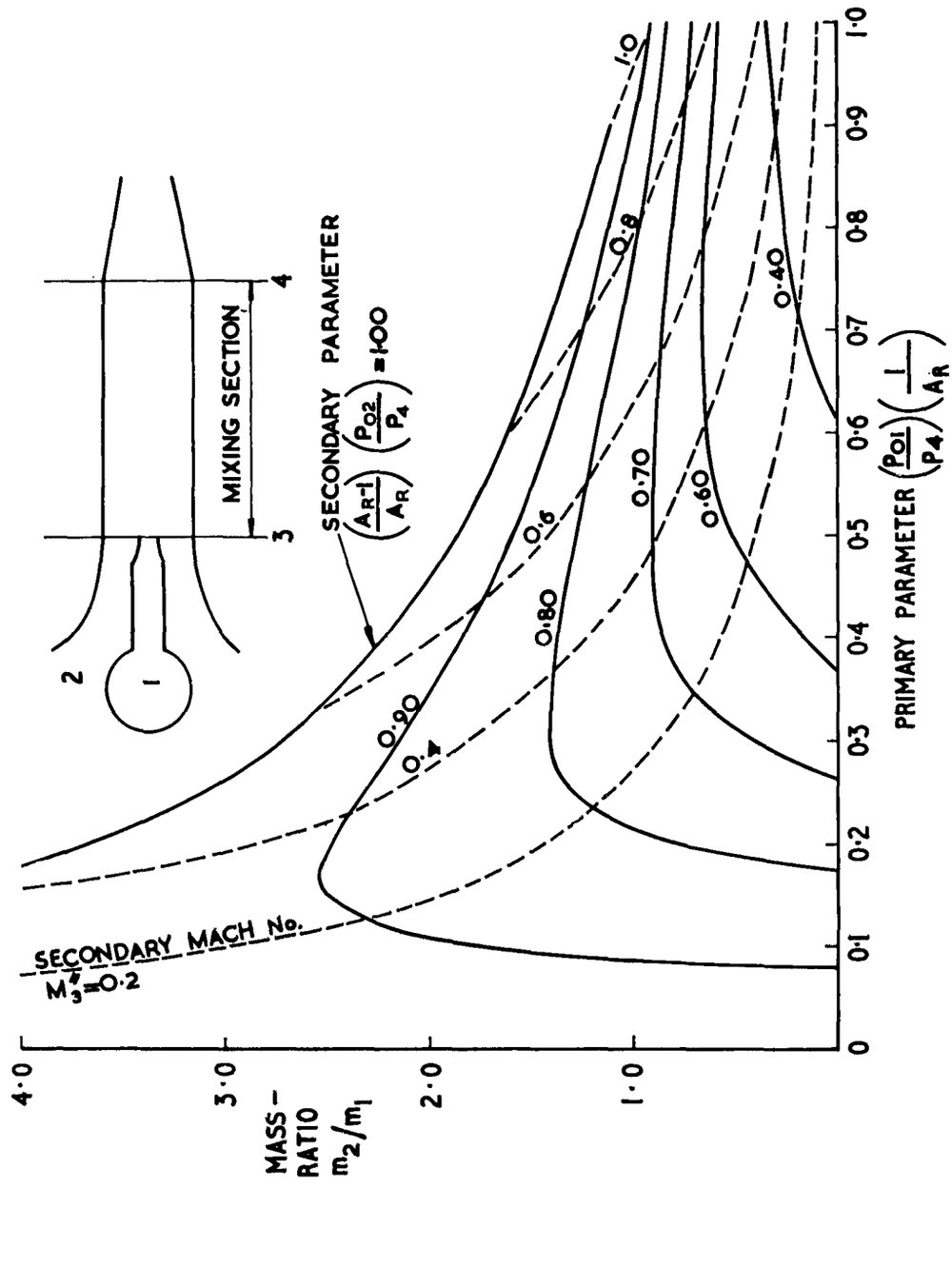

FIG. 13. THEORETICAL CURVES FOR INJECTOR MASS-FLOW RATIO.

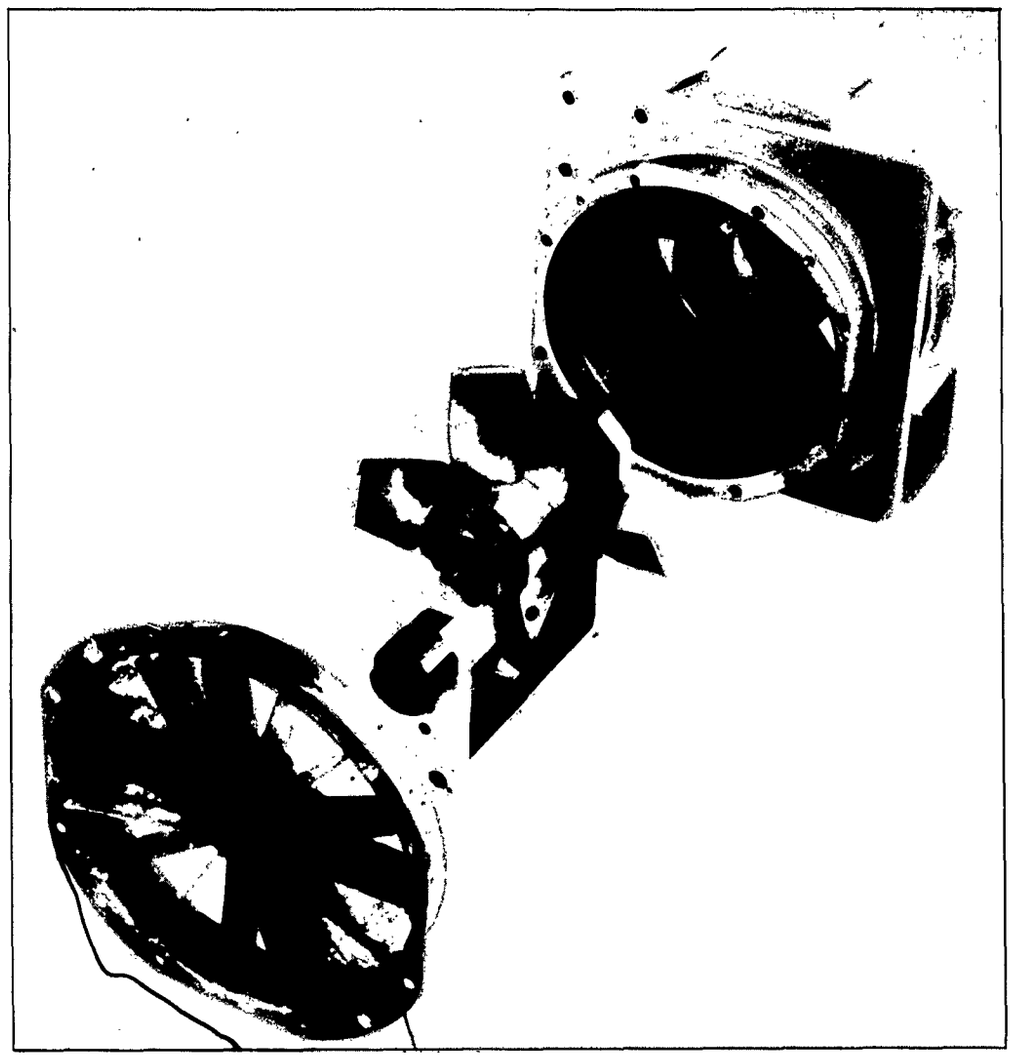

(a) 6in. DIAMETER MODEL FAN

FIG.14. DOWTY-ROTOL AIR DRIVEN FANS

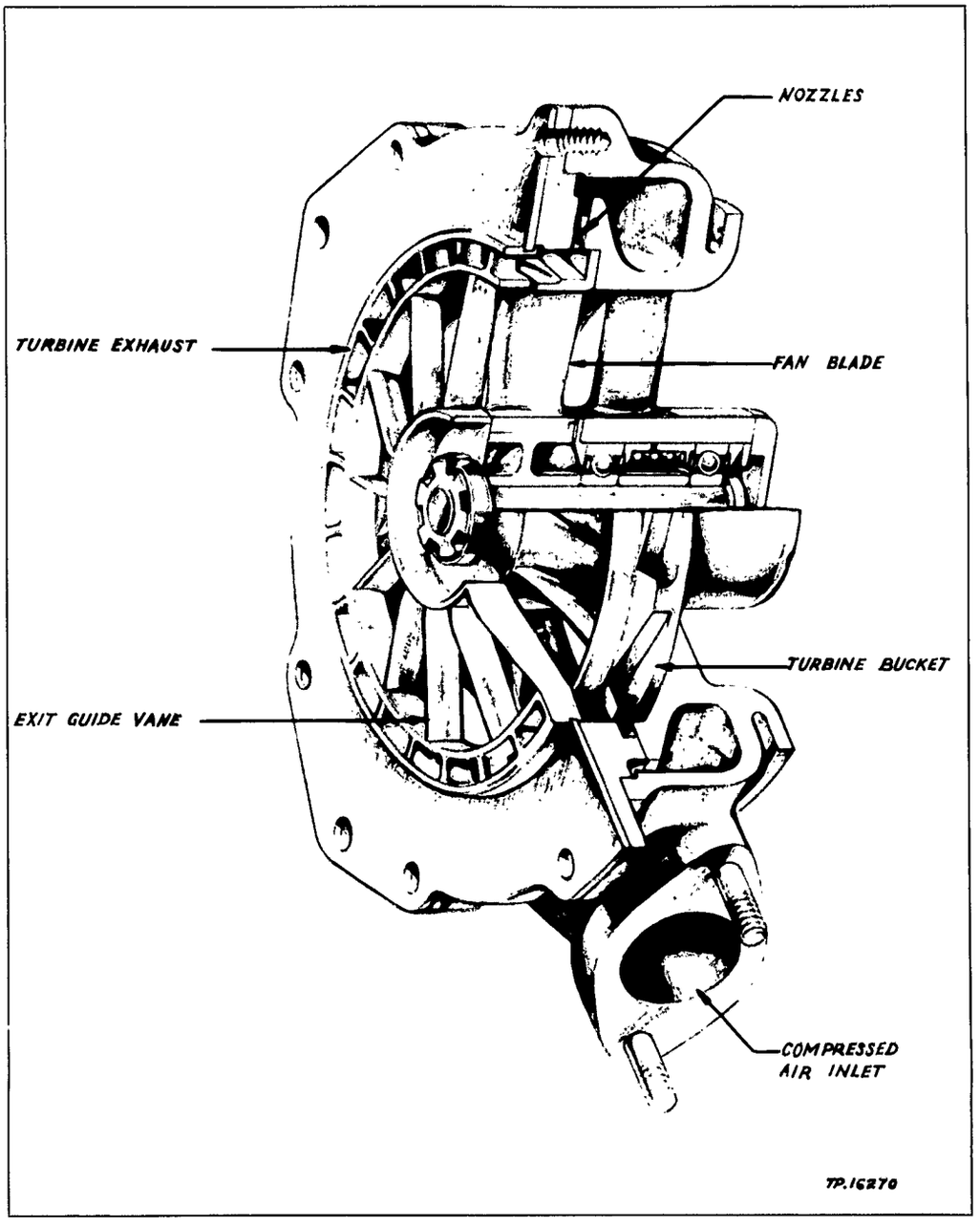

(b) 3in DIAMETER MODEL FAN

FIG.14.(Contd.) DOWTY-ROTOL AIR DRIVEN FANS

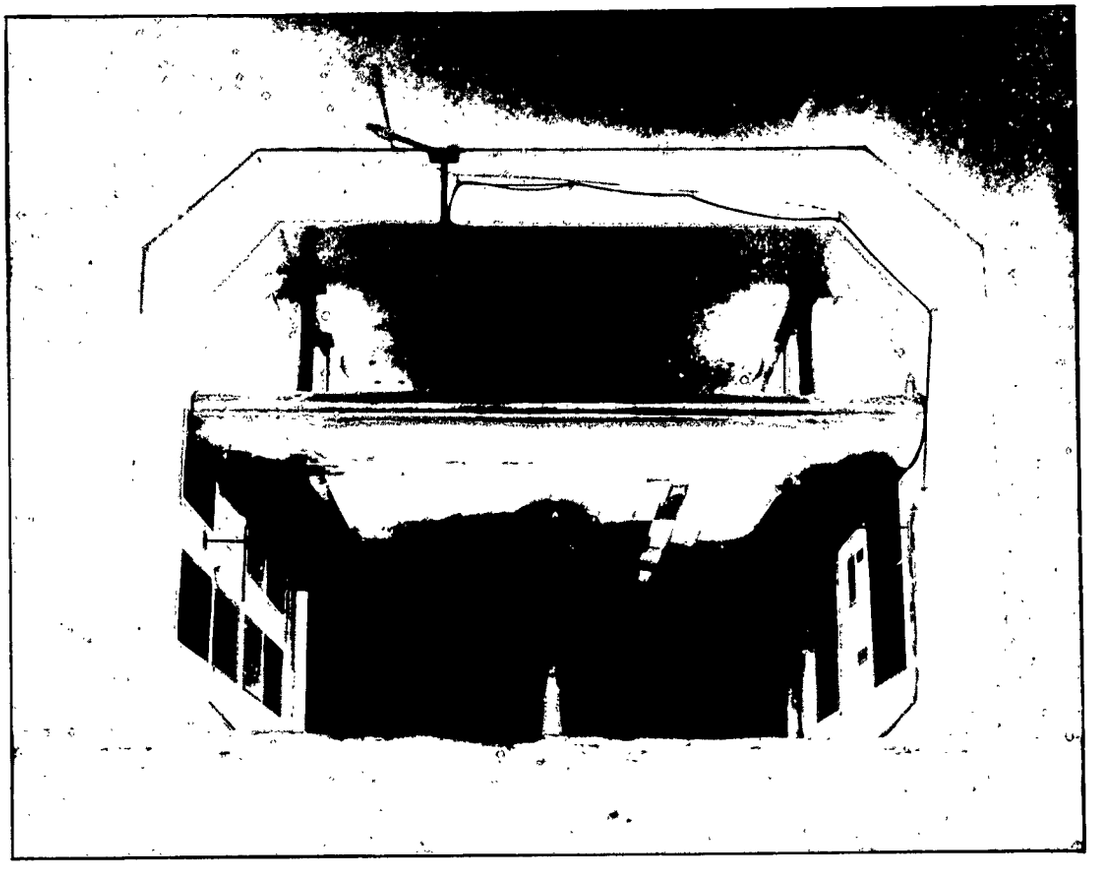

FIG.15. MOVING-BELT GROUND RIG IN R.A.E. 11½FT x 8½FT TUNNEL

R.A.E. 165330 64

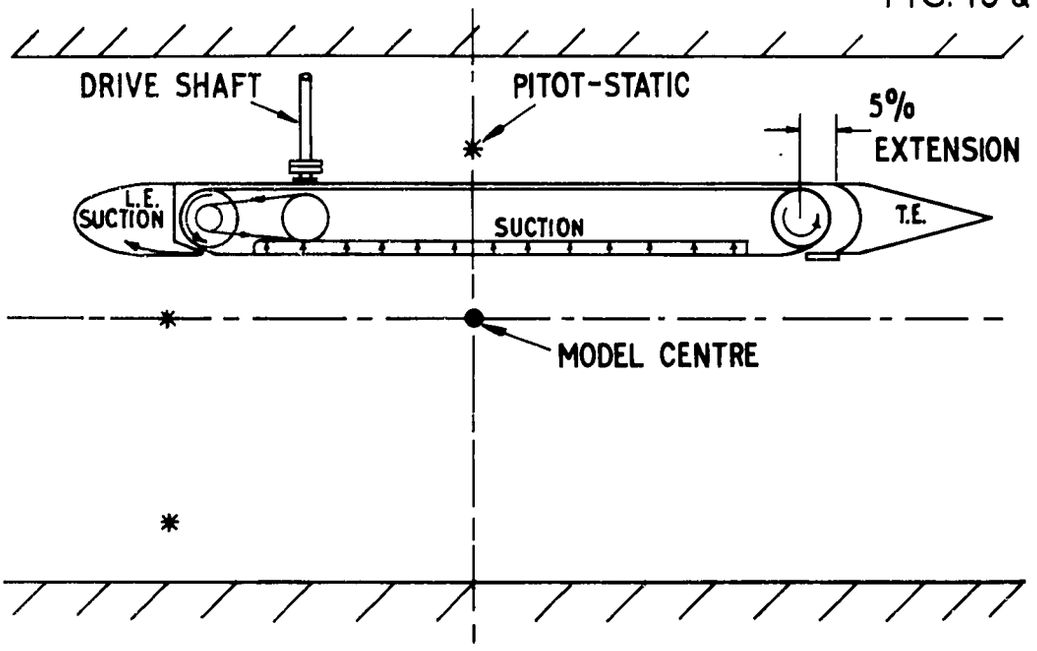

FIG. 16. SECTION OF MOVING-BELT GROUND RIG.

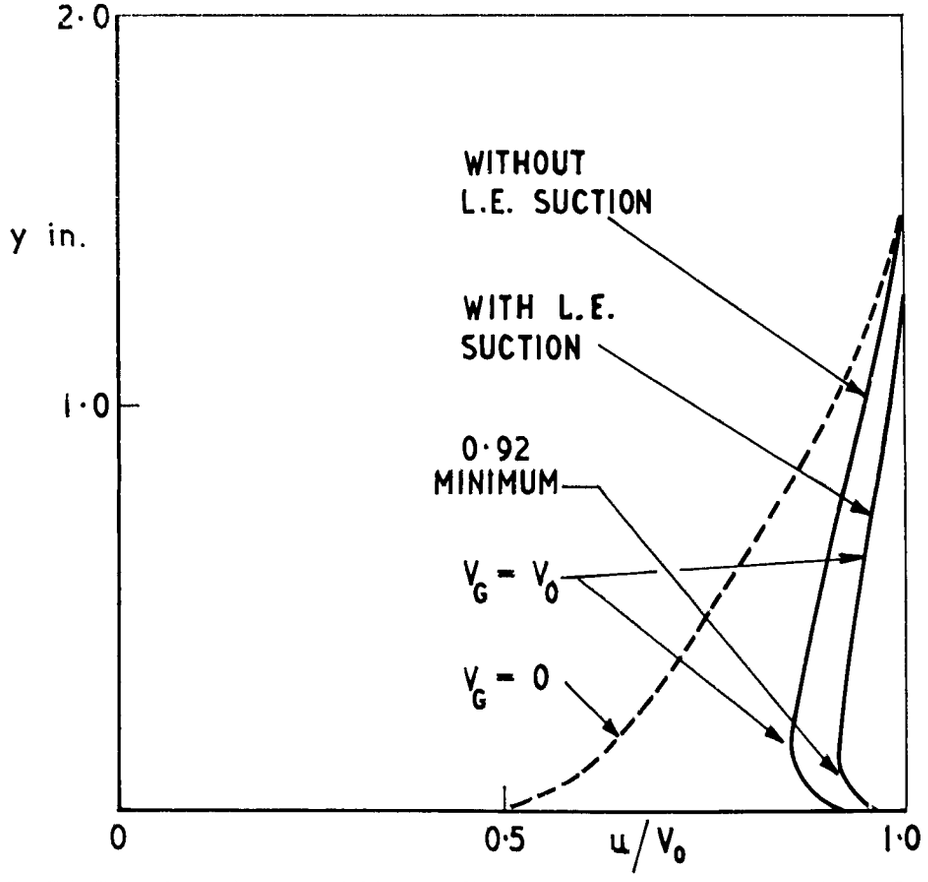

FIG. 17. GROUND BOUNDARY-LAYER PROFILES ON MOVING-BELT.

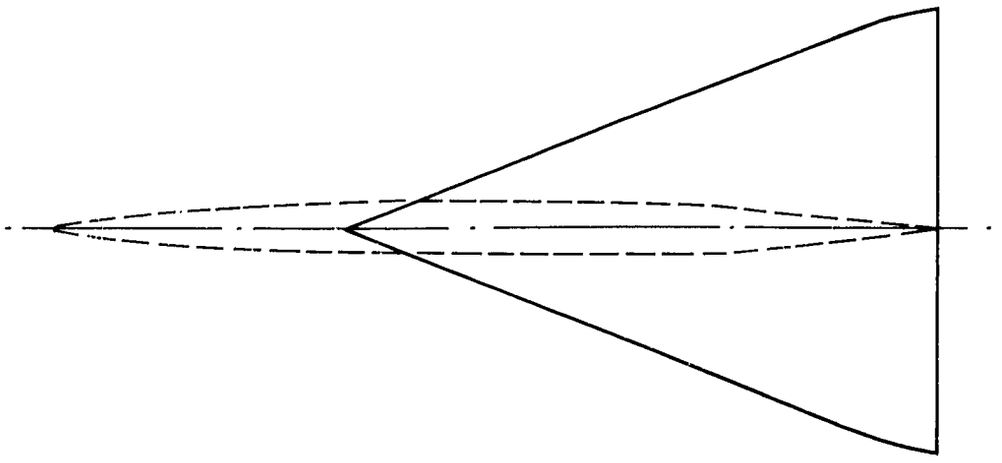

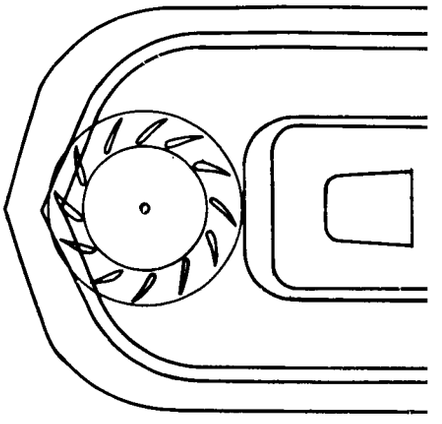

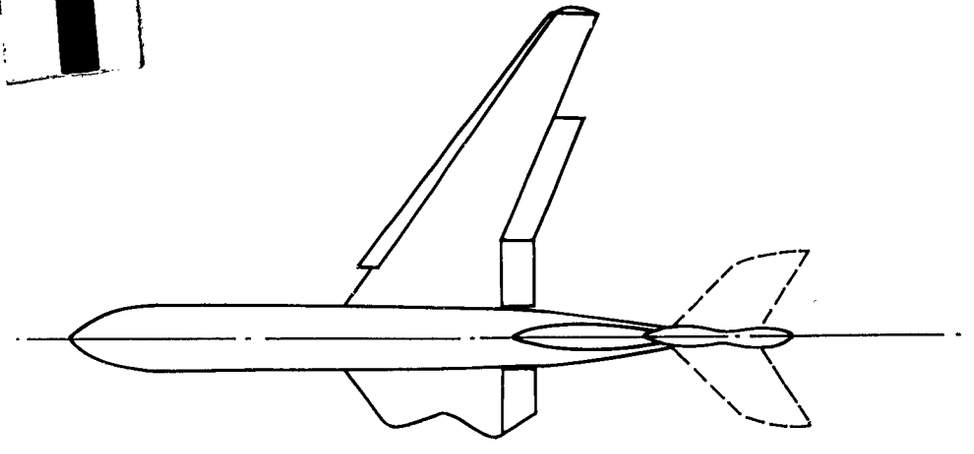

FIG.18. MODEL CONFIGURATIONS TESTED WITH

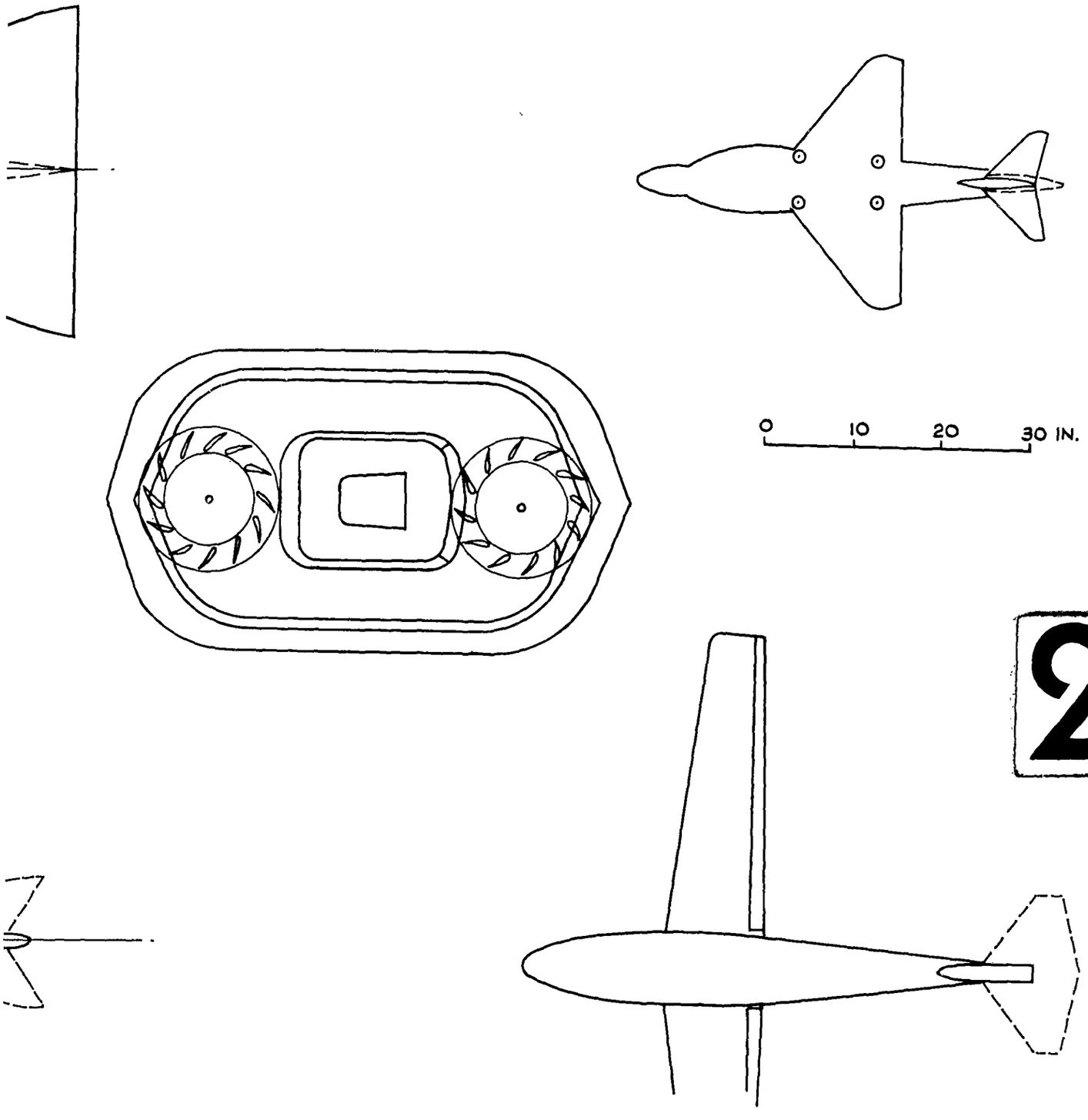

NFIGURATIONS TESTED WITH MOVING-BELT GROUND RIG.

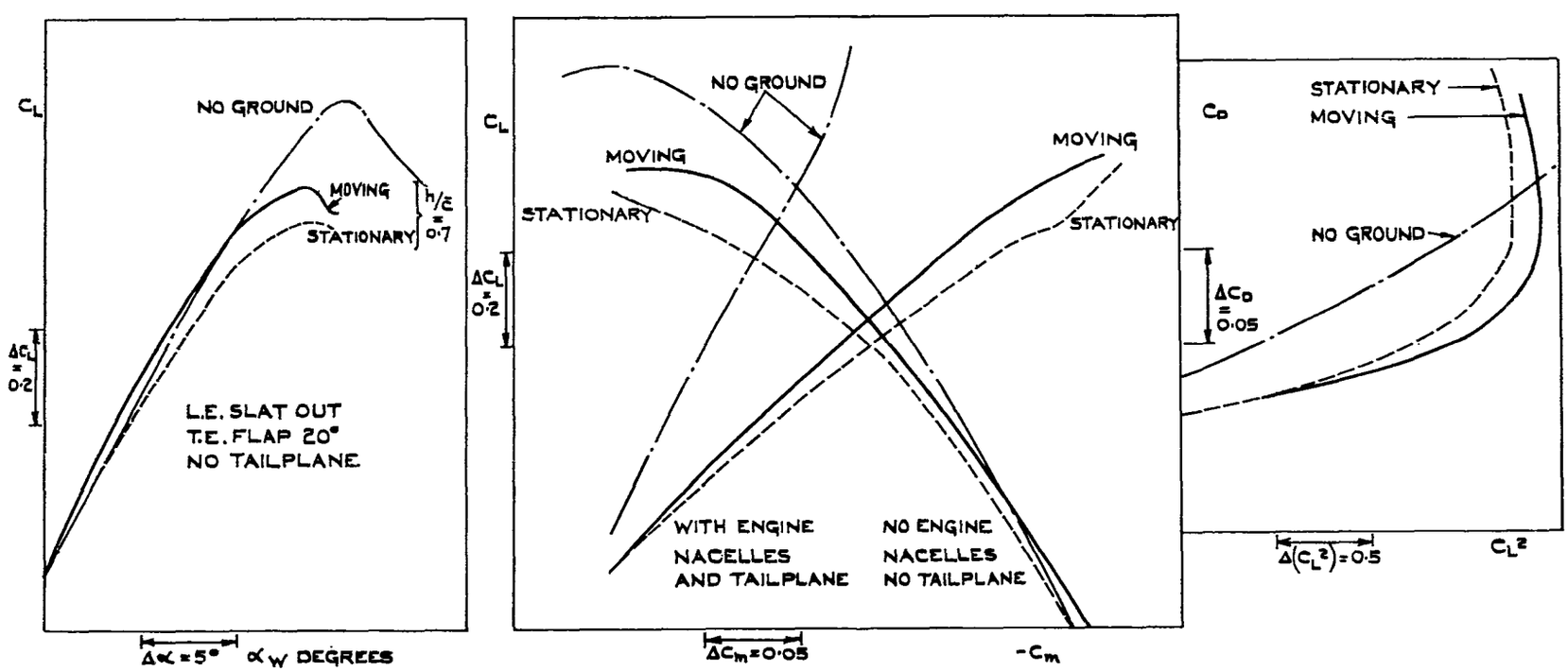

FIG. 19. GROUND EFFECT COMPARISONS FOR SUBSONIC JET-TRANSPORT CONFIGURATION.

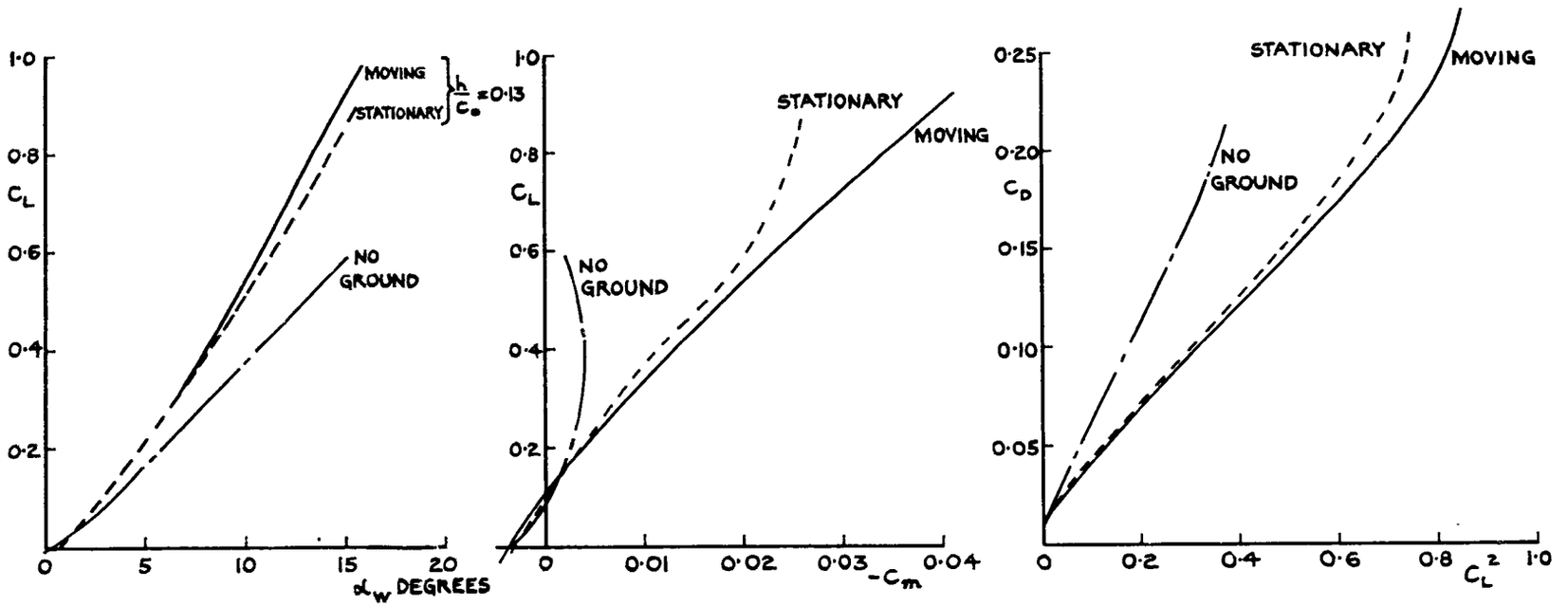

FIG.20. GROUND EFFECT COMPARISONS FOR SLENDER WING.

T.N. AERO. 2944.
FIG. 20.

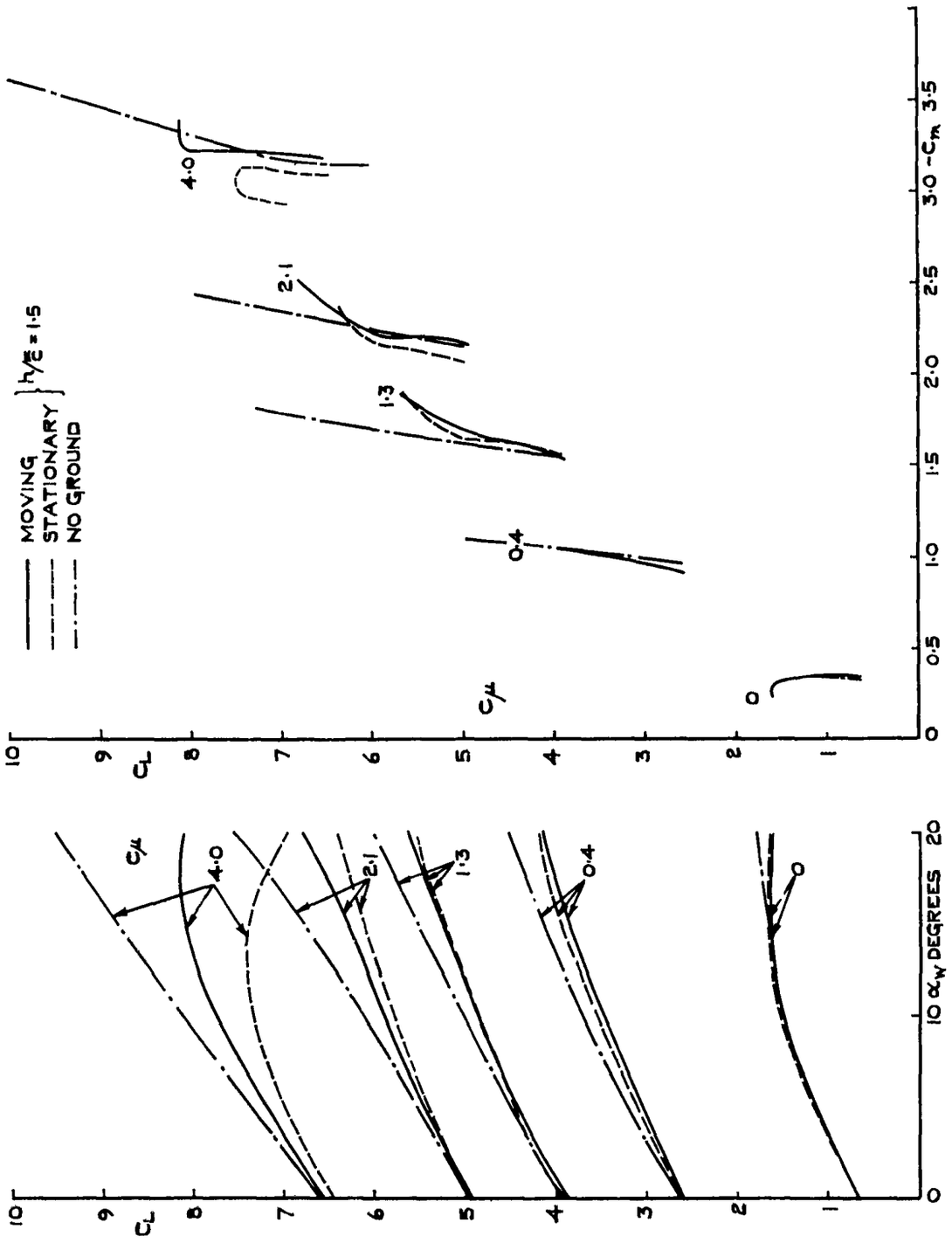

FIG. 21. GROUND EFFECT COMPARISONS FOR JET - FLAP WING.

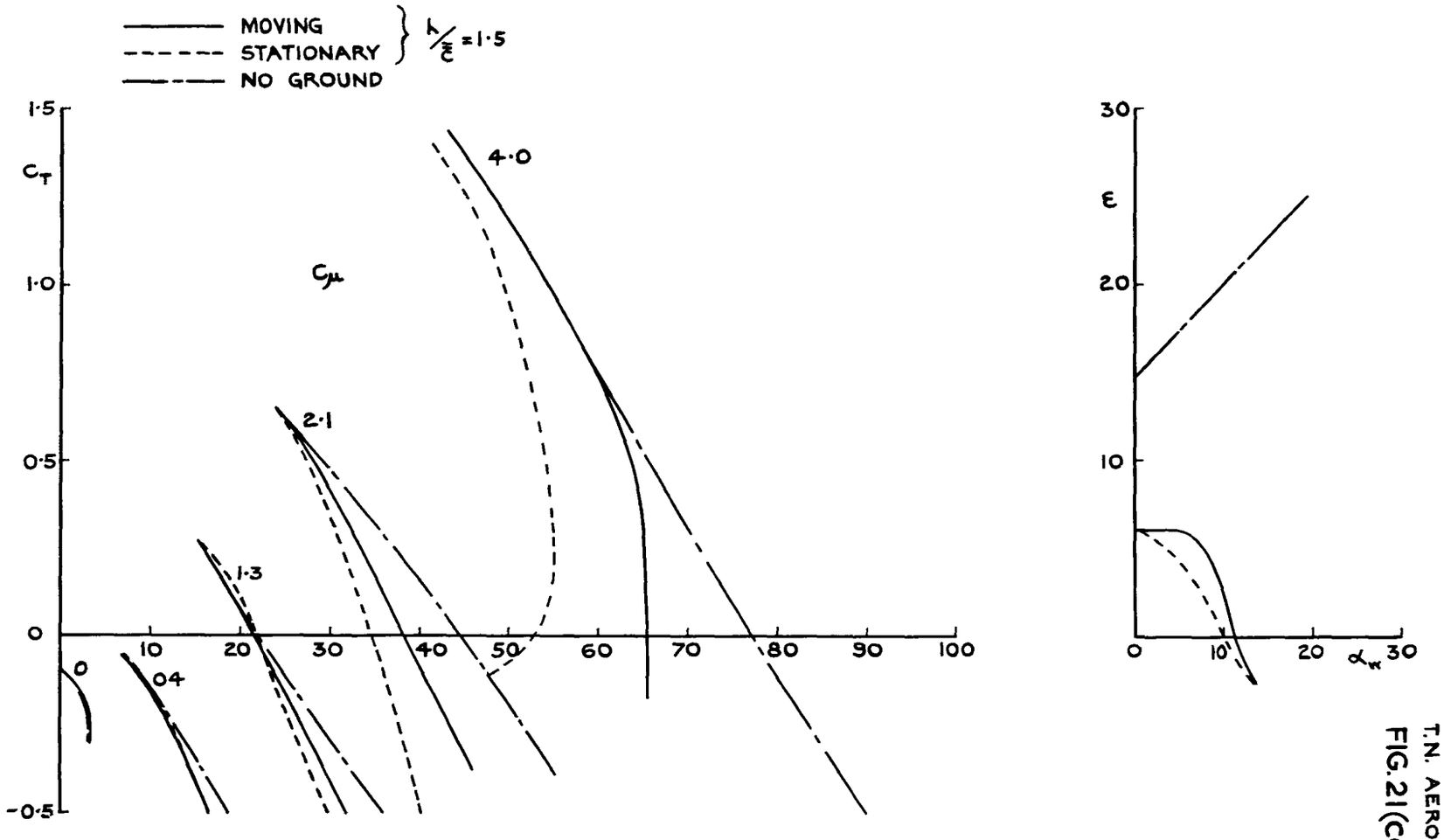

FIG. 21 (CONT'D.). GROUND EFFECT COMPARISONS FOR JET-FLAP WING.

T.N. AERO. 2944.
FIG. 21(CONT'D).

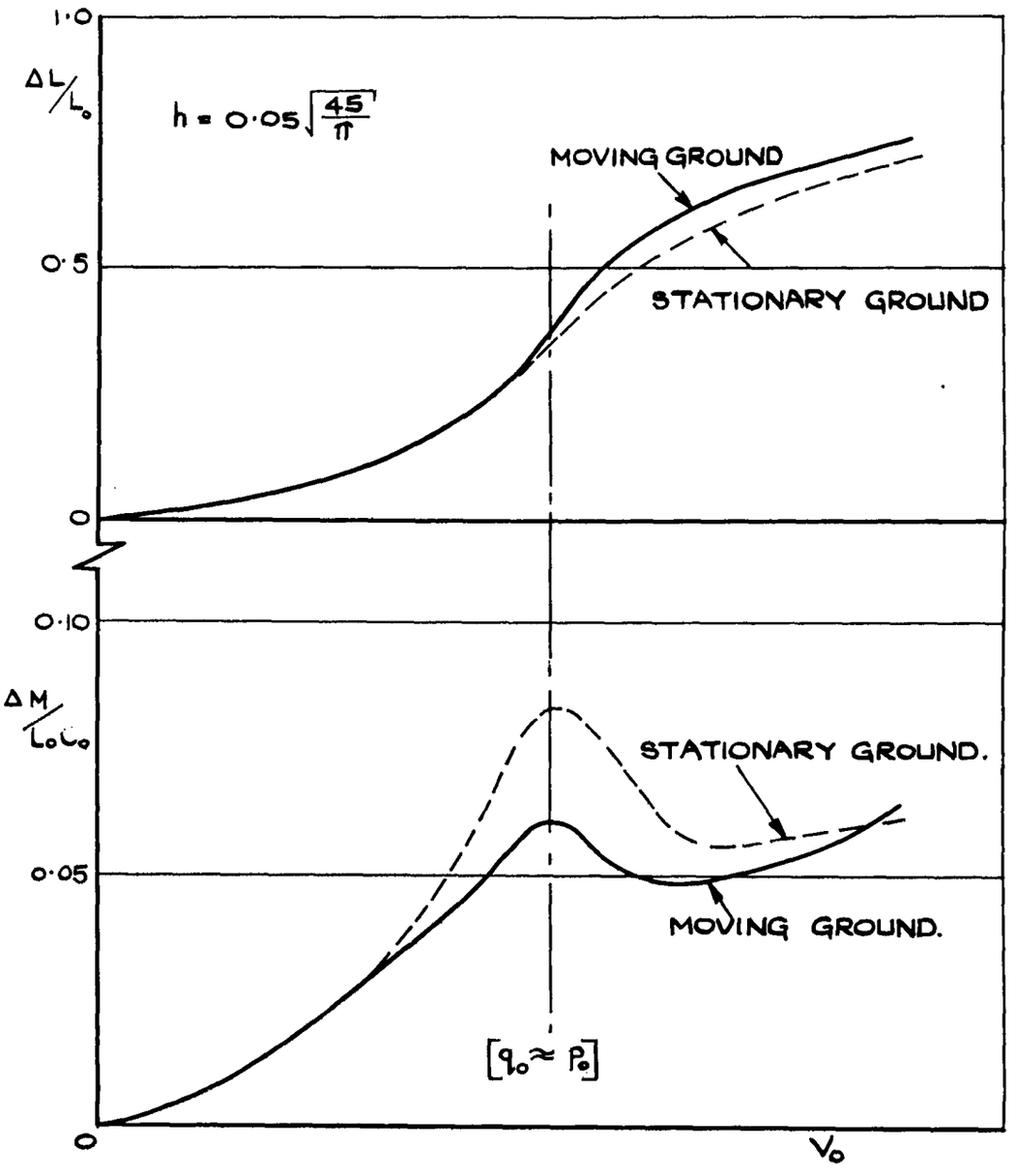

FIG. 22. GROUND EFFECT COMPARISONS FOR AIR-CUSHION VEHICLE.

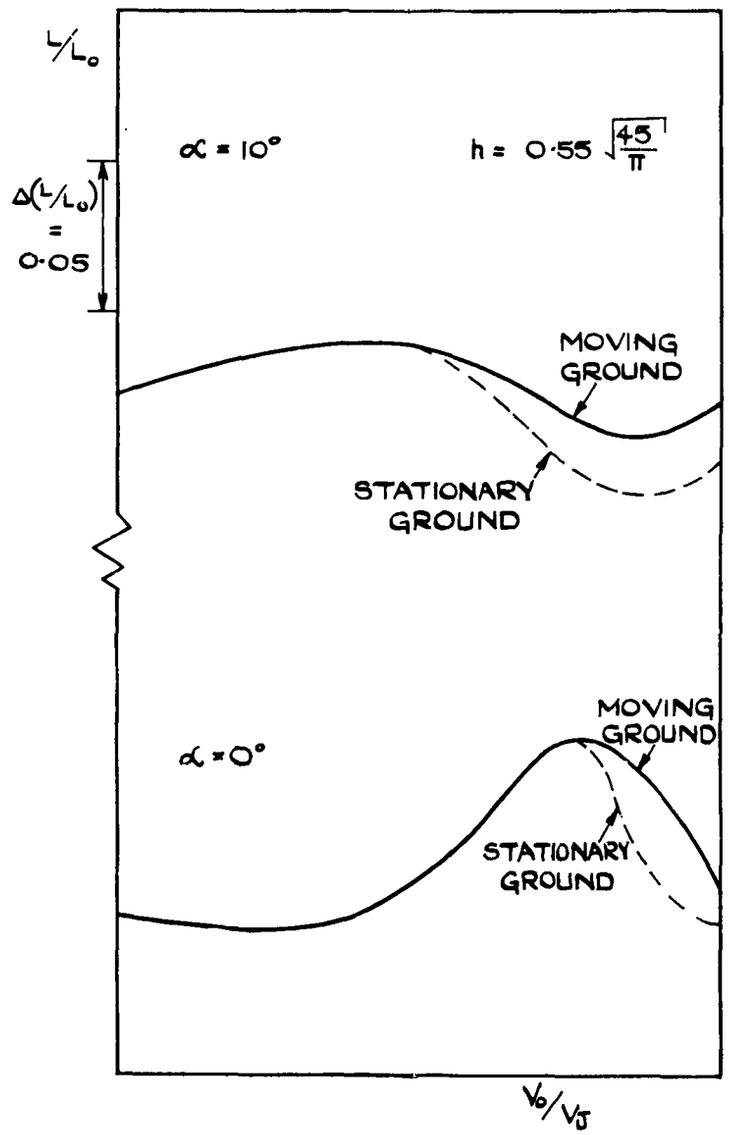

FIG. 23. GROUND EFFECT COMPARISONS FOR JET-LIFT MODEL.

UNCLASSIFIED

Technical Note No. Aero 2944 533.6.071.3:
Royal Aircraft Establishment 533.652.6

FURTHER DEVELOPMENTS IN LOW-SPEED WIND-TUNNEL TECHNIQUES FOR V/STOL AND HIGH-LIFT MODEL TESTING. Williams, J. and Butler, S.F.J. January 1964.

Experimental methods for wind-tunnel testing of high-lift models with boundary-layer control and circulation control were previously described by the authors about four years ago. Some of the further advances since then, particularly those to expedite investigations on jet and fan lift models at the Royal Aircraft Establishment (Farnborough and Bedford), are discussed in the present paper. Attention is mainly concentrated on the following three selected topics:-

UNCLASSIFIED (Over)

UNCLASSIFIED

Technical Note No. Aero 2944 533.6.071.3:
Royal Aircraft Establishment 533.652.6

FURTHER DEVELOPMENTS IN LOW-SPEED WIND-TUNNEL TECHNIQUES FOR V/STOL AND HIGH-LIFT MODEL TESTING. Williams, J. and Butler, S.F.J. January 1964.

Experimental methods for wind-tunnel testing of high-lift models with boundary-layer control and circulation control were previously described by the authors about four years ago. Some of the further advances since then, particularly those to expedite investigations on jet and fan lift models at the Royal Aircraft Establishment (Farnborough and Bedford), are discussed in the present paper. Attention is mainly concentrated on the following three selected topics:-

UNCLASSIFIED (Over)

UNCLASSIFIED

Technical Note No. Aero 2944 533.6.071.3:
Royal Aircraft Establishment 533.652.6

FURTHER DEVELOPMENTS IN LOW-SPEED WIND-TUNNEL TECHNIQUES FOR V/STOL AND HIGH-LIFT MODEL TESTING. Williams, J. and Butler, S.F.J. January 1964.

Experimental methods for wind-tunnel testing of high-lift models with boundary-layer control and circulation control were previously described by the authors about four years ago. Some of the further advances since then, particularly those to expedite investigations on jet and fan lift models at the Royal Aircraft Establishment (Farnborough and Bedford), are discussed in the present paper. Attention is mainly concentrated on the following three selected topics:-

UNCLASSIFIED (Over)

UNCLASSIFIED

Technical Note No. Aero 2944 533.6.071.3:
Royal Aircraft Establishment 533.652.6

FURTHER DEVELOPMENTS IN LOW-SPEED WIND-TUNNEL TECHNIQUES FOR V/STOL AND HIGH-LIFT MODEL TESTING. Williams, J. and Butler, S.F.J. January 1964

Experimental methods for wind-tunnel testing of high-lift models with boundary-layer control and circulation control were previously described by the authors about four years ago. Some of the further advances since then, particularly those to expedite investigations on jet and fan lift models at the Royal Aircraft Establishment (Farnborough and Bedford), are discussed in the present paper. Attention is mainly concentrated on the following three selected topics:-

UNCLASSIFIED (Over)

(a) Special mechanical and strain-gauge balance rigs for jet-blowing models;

(b) Engine exit and intake flow simulation at model scale;

(c) Ground simulation by a moving-belt rig.

The need, development and application of these techniques are considered, together with some problems still to be overcome.

UNCLASSIFIED

(a) Special mechanical and strain-gauge balance rigs for jet-blowing models;

(b) Engine exit and intake flow simulation at model scale;

(c) Ground simulation by a moving-belt rig.

The need, development and application of these techniques are considered, together with some problems still to be overcome.

UNCLASSIFIED

UNCLASSIFIED

(a) Special mechanical and strain-gauge balance rigs for jet-blowing models;

(b) Engine exit and intake flow simulation at model scale;

(c) Ground simulation by a moving-belt rig.

The need, development and application of these techniques are considered, together with some problems still to be overcome.

UNCLASSIFIED

[dstl]

Information Centre
Knowledge Services
[dstl] Porton Down
Salisbury
Wilts
SP4 0JQ
22060-6218
Tel: 01980-613753
Fax 01980-613970

Defense Technical Information Center (DTIC)
8725 John J. Kingman Road, Suit 0944
Fort Belvoir, VA 22060-6218
U.S.A.

AD#: AD00436352

Date of Search: 23 November 2009

Record Summary: AVIA 6/24459
Title: Further Developments in Low-Speed Wind-Tunnel Techniques for V/STOL and High-Lift Model Testing
Availability Open Document, Open Description, Normal Closure before FOI Act: 30 years
Former reference (Department): AERO 2944
Held by: The National Archives, Kew

This document is now available at the National Archives, Kew, Surrey, United Kingdom.

DTIC has checked the National Archives Catalogue website (http://www.nationalarchives.gov.uk) and found the document is available and releasable to the public.

Access to UK public records is governed by statute, namely the Public Records Act, 1958, and the Public Records Act, 1967.
The document has been released under the 30 year rule.
(The vast majority of records selected for permanent preservation are made available to the public when they are 30 years old. This is commonly referred to as the 30 year rule and was established by the Public Records Act of 1967).

This document may be treated as UNLIMITED.